zoosystema

2024 • 46 • 10

On one of the smallest Amazonian scorpions: a new species of *Microtityus* Kjellesvig-Waering, 1966 (Scorpiones, Buthidae) from Brazil, with amended diagnosis and potential distribution analysis for the genus

Jairo A. MORENO-GONZÁLEZ,
Rogério BERTANI & Leonardo S. CARVALHO

art. 46 (10) — Published on 25 April 2024
www.zoosystema.com

PUBLICATIONS SCIENTIFIQUES
MUSÉUM NAL HIST NATURELLE

Couverture / *Cover*:
Microtityus adriki n. sp., live habitus females, on leaf litter.

Zoosystema est indexé dans / Zoosystema *is indexed in:*
– Science Citation Index Expanded (SciSearch®)
– ISI Alerting Services®
– Current Contents® / Agriculture, Biology, and Environmental Sciences®
– Scopus®

Zoosystema est distribué en version électronique par / Zoosystema *is distributed electronically by:*
– BioOne® (http://www.bioone.org)

Les articles ainsi que les nouveautés nomenclaturales publiés dans *Zoosystema* sont référencés par / *Articles and nomenclatural novelties published in* Zoosystema *are referenced by:*
– ZooBank® (http://zoobank.org)

Zoosystema est une revue en flux continu publiée par les Publications scientifiques du Muséum, Paris / **Zoosystema** *is a fast track journal published by the Museum Science Press, Paris*

Les Publications scientifiques du Muséum publient aussi / *The Museum Science Press also publish:*
Adansonia, ***Geodiversitas***, ***Anthropozoologica***, ***European Journal of Taxonomy***, ***Naturae***, **Cryptogamie sous-sections *Algologie*, *Bryologie*, *Mycologie*, *Comptes Rendus Palevol*.**

Diffusion – Publications scientifiques Muséum national d'Histoire naturelle
CP 41 – 57 rue Cuvier F-75231 Paris cedex 05 (France)
Tél.: 33 (0)1 40 79 48 05 / Fax: 33 (0)1 40 79 38 40
diff.pub@mnhn.fr / https://sciencepress.mnhn.fr

ISSN (imprimé / *print*): 1280-9551/ ISSN (électronique / *electronic*): 1638-9387

On one of the smallest Amazonian scorpions: a new species of *Microtityus* Kjellesvig-Waering, 1966 (Scorpiones, Buthidae) from Brazil, with amended diagnosis and potential distribution analysis for the genus

Jairo A. MORENO-GONZÁLEZ
Division of Invertebrate Zoology, American Museum of Natural History New York, Central Park West at 79th Street, 10024-5192, New York City, NY (United States)
hansenochrus@gmail.com (corresponding author)

Rogério BERTANI
Laboratório de Ecologia e Evolução, Instituto Butantan, Avenida Dr. Vital Brasil, 1500, 05503-900, São Paulo, SP (Brazil)
bertani.rogerio@gmail.com

Leonardo S. CARVALHO
Universidade Federal do Piauí, Campus Amílcar Ferreira Sobral, BR 343, KM 3.5, Bairro Meladão, s/no. CEP 64808-660, Floriano, PI (Brazil)
carvalho@ufpi.edu.br

Submitted on 26 April 2023 | Accepted on 10 November 2023 | Published on 25 April 2024

urn:lsid:zoobank.org:pub:97472303-AA23-4E68-BD7F-1EE5CDA5BE20

Moreno-González J. A., Bertani R. & Carvalho L. S. 2024. — On one of the smallest Amazonian scorpions: a new species of *Microtityus* Kjellesvig-Waering, 1966 (Scorpiones, Buthidae) from Brazil, with amended diagnosis and potential distribution analysis for the genus. *Zoosystema* 46 (10): 245-268. https://doi.org/10.5252/zoosystema2024v46a10. http://zoosystema.com/46/10

ABSTRACT

A new scorpion species, *Microtityus adriki* n. sp., is described based on adult specimens collected in Cantá, state of Roraima (RR), northern Brazil. *Microtityus adriki* n. sp. is the second species of *Microtityus* Kjellesvig-Waering, 1966 known from Brazil and is one of the smallest scorpion species (12.39-19.47 mm) in the Amazonian region. In this study, we propose an amended generic diagnosis and a specific diagnosis, describe the male hemispermatophore of *Microtityus*, give the sequence of COI barcode, and present a potential distribution analysis for the genus. The morphology of the male hemispermatophore of *Microtityus* differs from that of other Neotropical buthid genera, except for the number of lobes (three lobes), which is a character state shared with several genera. The potential distribution model generated by MaxEnt suggests high environmental suitability for the genus in the Antilles and northern South America, with scattered high suitability in several regions of Central America. However, the model did not indicate high suitability in areas where Brazilian species occur (i.e., *Microtityus adriki* n. sp. and *Microtityus vanzolinii* Lourenço & Eickstedt, 1983), and this could be explained by a sampling bias. Therefore, future studies, including extensive sampling, are required to better understand the biogeographic processes behind the distribution of this genus.

KEY WORDS
Scorpion,
biogeography,
MaxEnt,
microbuthids,
niche,
Roraima,
new species.

RÉSUMÉ
Sur l'un des plus petits scorpions amazoniens : une nouvelle espèce de Microtityus *Kjellesvig-Waering, 1966 (Scorpiones, Buthidae) du Brésil, avec une diagnose amendée et une analyse de la distribution potentielle du genre.*
Une nouvelle espèce de scorpion, *Microtityus adriki* n. sp., est décrite sur la base de spécimens adultes collectés à Cantá, dans l'État de Roraima (RR), dans le nord du Brésil. *Microtityus adriki* n. sp. est la deuxième espèce de *Microtityus* Kjellesvig-Waering, 1966 connue au Brésil et constitue l'une des plus petites espèces de scorpions (12,39 à 19,47 mm) de la région amazonienne. Dans cette étude, nous proposons une diagnose générique amendée et une diagnose spécifique, décrivons l'hémi-spermatophore mâle de *Microtityus*, proposons la séquence de code-barres COI et une analyse de la distribution potentielle pour le genre. La morphologie de l'hémi-spermatophore mâle de *Microtityus* diffère de celle d'autres genres de buthidés néotropicaux, sauf pour le nombre de lobes (trois lobes), état de caractère partagé avec plusieurs genres. Le modèle de distribution potentielle généré par MaxEnt suggère une forte adéquation environnementale pour le genre dans les Antilles et le nord de l'Amérique du Sud, avec une adéquation élevée dispersée dans plusieurs régions d'Amérique centrale. Cependant, le modèle n'indique pas une adéquation élevée dans les zones où les espèces brésiliennes sont présentes (c'est-à-dire, *Microtityus adriki* n. sp. et *Microtityus vanzolinii* Lourenço & Eickstedt, 1983), ce qui pourrait s'expliquer par un biais d'échantillonnage. Par conséquent, des études futures, comprenant un échantillonnage approfondi, sont nécessaires pour mieux comprendre les processus biogéographiques à l'œuvre dans la distribution de ce genre.

MOTS CLÉS
Scorpion,
biogéographie,
MaxEnt,
microbuthids,
niche,
Roraima,
espèce nouvelle.

INTRODUCTION

Microtityus Kjellesvig-Waering, 1966 is a genus of small scorpions (< 25 mm) encompassing two subgenera (*Parvabsonus* Armas, 1974 and *Microtityus* Kjellesvig-Waering, 1966) and 41 species (40 extant and one fossil) (Table 1), distributed across the Antilles and northern South America (e.g. Fet & Lowe 2000; Botero-Trujillo & Noriega 2008; Botero-Trujillo *et al.* 2009; Armas & Teruel 2012). *Microtityus* species share some putative synapomorphies, such as a subtriangular carapace, five dorsal pedipalp patella trichobothria (d_1-d_5), a subpentagonal sternum, a female pectinal basal piece projected posteriorly, tergites I-VI with three to five distinct longitudinal carinae, and a telson with a large subaculear tubercle (Kjellesvig-Waering 1966; Sissom 1990; Botero-Trujillo & Noriega 2008; Teruel & Kovařík 2012). Nevertheless, a comparative diagnosis for the genus is lacking, the male hemispermatophore is unknown, and no phylogenetic hypothesis has been proposed to test the monophyly or phylogenetic relationships of *Microtityus* and its species and subgenera (Fet & Lowe 2000; Botero-Trujillo & Noriega 2008; Botero-Trujillo *et al.* 2009).

In northern South America, 11 *Microtityus* species have been described from Brazil, Colombia and Venezuela (Table 1). Among these countries, Brazil has the lowest number of *Microtityus* records, totaling two. One corresponds to *Microtityus vanzolinii* Lourenço & Eickstedt 1983, a species described from two female specimens collected in Igarapé Urumutum, near Barcelos, state of Amazonas (Lourenço & Eickstedt 1983), and the other to a single male *Microtityus* collected in an unspecified locality in the state of Mato Grosso (González-Sponga 2001). Despite the sampling efforts spanning the last 40 years, carried out across numerous localities within the Brazilian Amazon, which led to the discovery of numerous taxa in the families Buthidae (e.g. *Ananteris* Thorell, 1891; *Tityus* C.L. Koch, 1836) and Chactidae (e.g. *Brotheas* C.L. Koch, 1837; *Broteochactas* Pocock, 1893; *Chactopsis* Kraepelin, 1912; *Teuthraustes* Simon, 1878) (Lourenço 2004, 2005, 2017; Lourenço *et al.* 2011), no additional *Microtityus* specimens have ever been collected.

In contrast, over 50% of the known *Microtityus* species have been described from countries such as Cuba (10 sp.) and the Dominican Republic (13 sp.) (Table 1). Given the numerous species described within these relatively small countries and taking into account the significant biodiversity shortfalls prevalent in northern South America, it is highly likely that more species will be discovered in the forested biomes of this region as sampling efforts intensify (Botero-Trujillo & Noriega 2008). Therefore, decreasing the sampling bias across the Amazon forest will probably yield additional *Microtityus* species in the forthcoming years.

In this contribution, we describe a new species of *Microtityus* from the state of Roraima, northern Brazil. With the addition of this species, the number of living species within this genus has increased to 42. Additionally, we propose an amended generic diagnosis and a specific diagnosis for the new species, describe the male hemispermatophore of *Microtityus*, give the sequence of COI barcode, and present potential distribution modeling for the genus. The potential distribution approach aimes to identify areas most likely to harbor hitherto unknown *Microtityus* species and/or populations.

MATERIAL AND METHODS

Material

The examined material is housed at the following Brazilian biological collections: Instituto Nacional de Pesquisas da Amazônia (INPA, curator Marcio Luiz de Oliveira); Museu Nacional, Universidade Federal do Rio de Janeiro, Rio de Janeiro (MNRJ, curator Adriano Kury); Museu de Zoologia da Universidade

Table 1. — List of species of *Microtityus* Kjellesvig-Waering, 1966 and their distribution.

n	Species	Distribution
1	*Microtityus adriki* n. sp.	Brazil: state of Roraima
2	*Microtityus ambarensis* Schawaller 1982	Dominican Republic: unknown
3	*Microtityus angelaerrosae* González-Sponga, 2001	Venezuela: Aragua state
4	*Microtityus barahona* Armas & Teruel, 2012	Dominican Republic: Barahona and Independencia departments
5	*Microtityus biordi* González-Sponga, 1970	Venezuela: Miranda state
6	*Microtityus bivicentorum* Botero-Trujillo, Erazo-Moreno & Pérez, 2009	Colombia: Cesar department
7	*Microtityus borincanus* Teruel, Rivera & Sánchez, 2014	Puerto Rico: Sabana Grande municipality
8	*Microtityus capayaensis* González-Sponga, 2001	Venezuela: Miranda state
9	*Microtityus consuelo* Armas & Marcano Fondeur, 1987	Dominican Republic: La Romana, Monte Plata and San Pedro de Macorís provinces
10	*Microtityus desuzeae* González-Sponga, 2001	Venezuela: Aragua state
11	*Microtityus difficilis* Teruel & Armas, 2006	Cuba: Holguín province
12	*Microtityus dominicanensis* Santiago-Blay, 1985	Dominican Republic: Peravia, San Cristóbal, and San José de Ocoa provinces
13	*Microtityus eustatia* Armas, 2018	British Virgin Islands: Eustatia, Virgin Gorda and Great Camanoe Islands
14	*Microtityus farleyi* Teruel, 2000	Cuba: Guantánamo province
15	*Microtityus flavescens* Teruel, 2001	Cuba: Santiago de Cuba province
16	*Microtityus franckei* Botero-Trujillo & Noriega, 2008	Colombia: Magdalena department
17	*Microtityus fundorai* Armas, 1974	Cuba: Holguín and Santiago de Cuba provinces
18	*Microtityus guantanamo* Armas, 1984	Cuba: Guantánamo province
19	*Microtityus iviei* Armas, 1999	Dominican Republic: Barahona and Pedernales provinces
20	*Microtityus jaumei* Armas, 1974	Cuba: Santiago de Cuba province
21	*Microtityus joseantonioi* González-Sponga, 1981	Venezuela: Anzoátegui state
22	*Microtityus kovariki* Teruel & Infante, 2007	Cuba: Granma province
23	*Microtityus lantiguai* Armas & Marcano Fondeur, 1992	Dominican Republic: Pedernales province
24	*Microtityus litoralensis* González-Sponga, 2001	Venezuela: Vargas state
25	*Microtityus lourenco*i Armas & Teruel, 2012	Dominican Republic: La Altagracia province
26	*Microtityus minimus* Kovařík & Teruel, 2014	Dominican Republic: Azua province
27	*Microtityus paucidentatus* Armas & Marcano Fondeur, 1992	Dominican Republic: Bahoruco province
28	*Microtityus prendinii* Armas & Teruel, 2012	Dominican Republic: Samaná province
29	*Microtityus pusillus* Teruel & Kovařík, 2012	Cuba: Santiago de Cuba province
30	*Microtityus reini* Armas & Teruel, 2012	Dominican Republic: Peravia province
31	*Microtityus rickyi* Kjellesvig-Waering, 1966	Trinidad and Tobago: Teteron Bay and Port-of-Spain
32	*Microtityus santosi* Teruel, Rivera & Sánchez, 2014	Puerto Rico: Culebra municipality
33	*Microtityus sevciki* González-Sponga, 2001	Venezuela: Aragua state
34	*Microtityus solegladi* Armas & Teruel, 2012	Dominican Republic: Bahoruco and Independencia provinces
35	*Microtityus starri* Lourenço & Huber, 1999	Trinidad and Tobago: Little Tobago
36	*Microtityus trinitensis* Armas, 1974	Cuba: Cienfuegos, Trinidad, and Holguín provinces
37	*Microtityus vanzolinii* Lourenço & Eickstedt, 1983	Brazil: Amazonas state
38	*Microtityus vieques* Teruel, Rivera & Santos, 2015	Puerto Rico: Vieques Island
39	*Microtityus virginiae* Armas, 1999	Dominican Republic: Independencia province
40	*Microtityus vulcanicus* Teruel, 2019	Cuba: Guantánamo province
41	*Microtityus waeringi* Francke & Sissom, 1980	United States: Virgin Islands
42	*Microtityus yaracuyanus* González-Sponga, 2001	Venezuela: Yaracuy state

de São Paulo (MZSP, curator R. Pinto-da-Rocha), the Cryo Collection of the Laboratory of Evolution and Systematics of Arachnids (IBALCC-RPDR, curator Ricardo Pinto-da-Rocha) and Coleção de História Natural da Universidade Federal do Piauí, Floriano (CHNUFPI, curator J. F. Vilela).

Morphology

Specimens were studied under a Leica M125 stereoscope with a trinocular tube. Z-stack images under white and UV lights, as well as measurements, were obtained using a Leica M205C stereomicroscope with a DFC 450 camera attached, combined with Leica LAS Montage and LAS 3D modules. Picture parameters such as brightness and contrast were edited with GIMP (GNU Image Manipulation Program) (www.gimp.org/). Figures were composed with Inkscape 0.91 (www.inkscape.org/).

The general terminology follows Stahnke (1970) and Sissom *et al.* (1990). Pedipalp carinae nomenclature follows Prendini (2000) and metasomal carinae nomenclature follows Ochoa *et al.* (2010). The cheliceral dentition of Buthidae follows Vachon (1963) and trichobothrial terminology follows Vachon (1974, 1975). The sternum nomenclature follows Soleglad & Fet (2003) and the ocelli nomenclature follows Loria & Prendini (2014).

Molecular data

We extracted genomic DNA from leg tissues using the protocol of Fetzner (1999) and kept voucher specimen in the IBALCC-RPDR. The extraction was quantified using a Thermo Scientific Nanodrop spectrophotometer. Genomic DNA was then used as a template to amplify COI using degenerate primers (LCO1490-jj2 5'- CHACWAAYCAYAARGAYATYGG and

HCO2198-jj2 5'-ANACTTCNGGRTGNCCAAARAATCA), following the protocol described by Pinto-da-Rocha *et al.* (2014). PCR reaction with a volume of 25 µL contains 13.95 µL Milli-Q H2O, 5 µL PCR buffer (Fermentas®), 2 µL MgCl2, 1 µL dNTPs (80 µM) (Fermentas®), 1 µL primer (0.4 µM) of each primer, and 0.05 µL GoTaq DNA polymerase (Fermentas®). We conducted a touch-down PCR reaction with the parameters described by Astrin *et al.* (2016).

PCR amplification was observed using electrophoresis of agarose gel (2% agarose). The amplified product was purified using Agencourt Ampure XP (Beckman Coulter), then quantified using a Thermo Scientific NanoDrop spectrophotometer. We prepared the sequencing reaction with the BigDye® Terminator v3.1 Cycle Sequencing Kit (Applied Biosystems), precipitated the PCR product with sodium acetate, and sequenced it using an ABI PRISM® 3100 Genetic Analyser/HITACHI (Applied Biosystems). Sequence editing (e.g., primer trimming) and contiguous sequence were generated from AB1 files using Geneious R11 (http://www.geneious.com). The consensus sequence was checked against the NCBI nucleotide database using the BLAST algorithm to detect possible contaminations. The consensus was inspected in Geneious to detect potential stop codons.

Niche modeling analyses

A distribution database, including records of all described *Microtityus* species, was compiled from a literature review of all taxonomic papers on this genus (Appendix 1). Records without coordinates were georeferenced *a posteriori* using Google Earth Pro 7.3.3 or relevant literature (e.g. Rojas-Runjaic & Sousa 2007). A distribution map was produced by plotting the georeferenced localities onto a Natural Earth surface cover raster (https://www.naturalearthdata.com/downloads/10m-natural-earth-2/10m-natural-earth-2-with-shaded-relief-water-and-drainages/), using ArcGIS 10.3 (Environmental Systems Research Institute, Redlands, CA). All rasters were plotted using stretched symbology with 2.5 standard deviations. The biogeographic regionalisation of the Neotropical region follows Morrone (2017).

As representatives of *Microtityus* are rare in Brazil, we conducted a qualitative exploratory analysis to search for areas with high suitability for *Microtityus*, using species distribution modeling (SDM) based on our occurrence record database (Appendix 1). This analysis disregards individual species environmental thresholds and considers all *Microtityus* as a single biological entity in the model inputs. This was required as none of them presented enough individual records to allow separate analyses. As predictors, the 19 climatic variables available in the WorldClim 2 (https://www.worldclim.org/data/index.html) database were used, in addition to mean tree density (Crowther *et al.* 2015) and mean canopy height (Simard *et al.* 2011), both at the 1 km^2 scale (see Table 3). To remove the spatial autocorrelation between the predictor layers, a principal component analysis (PCA) was carried out in the software Dinamica Ego 6, using the package 'BioDinamica' (Oliveira *et al.* 2019).

The PCAs whose proportion of variance was higher than expected by chance (i.e., for 21 predictor variables, each one is expected to explain *c.* 4.76% of the variance by chance) were used as predictors in the modeling (see Tables 4-6). The SDM was carried out using the MaxEnt algorithm, without applying a threshold rule, with 500 maximum interactions, a random test percentage of 25%, raw output formatted, 15 bootstrap replicates, and removing duplicates from the same grid cell (following recommendations by Merow *et al.* [2013]). Additionally, the environmental niche occupied by the two Brazilian species and the non-Brazilian taxa was compared using the same SDM predictors, following the protocol described by Santos-da-Silva *et al.* (2017).

Abbreviations

Carinae and positions

D	digital;
DE	dorsoexternal;
DI	dorsointernal;
DL	dorsolateral;
DM	dorsomedian;
DMA	dorsomarginal;
DS	dorsal secondary;
DSM	dorsosubmedian;
EM	externomedian;
ES	external secondary;
IM	internomedian;
LIM	lateral inframedian;
ML	median lateral;
SA	secondary accessory;
VE	ventroexternal;
VI	ventrointernal;
VL	ventrolateral;
VM	ventromedian;
VSM	ventrosubmedian.

Hemispermatophore

B	body;
Bl	basal lobe;
El	external lobe;
F	foot;
Fl	flagellum;
il	internal lobe;
Prec	pars recta;
Prex	pars recta expansion;
Pref	pars reflexa.

Ocelli

ALMa	anterolateral major ocellus;
ADMi	anterodorsal minor ocellus;
MLMa	mediolateral major ocellus;
PLMa	posterolateral major ocellus.

Institutions

CHNUFPI	Coleção de História Natural da Universidade Federal do Piauí, Floriano;
IBALCC-RPDR	Cryo Collection of the Laboratory of Evolution and Systematics of Arachnids, São Paulo;
INPA	Instituto Nacional de Pesquisas da Amazônia, Manaus;
MNRJ	Museu Nacional do Rio de Janeiro, Rio de Janeiro;
MZSP	Museu de Zoologia da Universidade de São Paulo, São Paulo.

SYSTEMATICS

Family Buthidae C.L. Koch, 1837

Genus *Microtityus* Kjellesvig-Waering, 1966

Microtityus Kjellesvig-Waering, 1966: 130.

Type species. — *Microtityus rickyi* Kjellesvig-Waering, 1966 by original designation.

Included species. — Forty-two species (Table 1).

Distribution. — Northern South America (Brazil, Colombia, Venezuela) and the Caribbean (British Virgin Islands, Cuba, Dominican Republic, Puerto Rico, Trinidad and Tobago, Virgin Islands [United States]). See Figure 10A, Table 1 and Appendix 1.

Amended diagnosis. — Among the buthid genera of the Americas, *Microtityus* shares the presence of telotarsi I-IV with ventral setae distributed in two submedian rows with *Alayotityus* (Armas, 1973); *Chaneke* (Francke, Teruel & Santibáñez-López, 2014); *Heteroctenus* Pocock, 1893; *Ischnotelson* (Esposito, Yamaguti, Souza, Pinto-da-Rocha & Prendini, 2017); *Jaguajir* (Esposito, Yamaguti, Souza, Pinto-da-Rocha & Prendini, 2017); *Tityopsis* (Armas, 1974); *Tityus* (C. L. Koch, 1836) [in part]; *Troglorhopalurus* (Lourenço, Baptista & Giupponi, 2004), and *Zabius* (Thorell, 1893).
However, *Microtityus* may be readily recognized from these genera based on the presence of: 1) a subtriangular carapace with an anterior margin strongly narrowed compared to the posterior margin (Fig. 2A, B); 2) tergites I-VI each with three (Fig. 2A, B) to five dorsal carinae; 3) a subpentagonal sternum (Fig. 5A, B); and 4) a female pectinal plate strongly projected posteriorly (Fig. 5B). Whereas, the other genera share: 1) a trapezoidal carapace with an anterior margin slightly to moderately narrowed compared with the posterior margin; 2) tergites I-VI with three carinae (*Alayotityus*, *Ischnotelson* and *Zabius*) or a single carina (*Chaneke*, *Heteroctenus*, *Jaguajir*, *Tityus*, *Tityopsis* and *Troglorhopalurus*); 3) a subtriangular sternum; and 4) a female pectinal plate not projected (*Chaneke*, *Heteroctenus* [in part], *Ischnotelson*, *Jaguajir* [in part], *Tityus*, *Troglorhopalurus* and *Zabius*) or slightly projected posteriorly (*Heteroctenus* [in part] and *Jaguajir* [in part]).

Microtityus adriki n. sp.
(Figs 1-11; Tables 1; 2; Appendix 1)

urn:lsid:zoobank.org:act:006BC5B2-EF98-44AB-85DB-2B8D3C6CCF29

Type material. — **Holotype. Brazil** • 1 ♀; state of Roraima, Cantá; 2°36'51.11"N, 60°36'29.9"W; 137 m a.s.l.; 30.VI.2018; F. F. Xavier, R. Bertani and M. Q. Almeida leg.; MZSP 76547.
Paratypes. Brazil • 3 ♂; state of Roraima, Cantá; 2°36'51.11"N, 60°36'29.9"W; 137 m a.s.l.; 30.VI.2018; F. F. Xavier, R. Bertani and M. Q. Almeida leg.; INPA-SCO 00623, MNRJ 7685, MZSP 76548 • 1 ♀; same data; INPA-SCO 00624 • 3 ♀; same data; MNRJ 7685 • 2 ♀; same data; MZSP 76549 • 2 ♂; state of Roraima, Cantá, on the side of the BR432 road (around 10 km away from the city of Cantá); 2°35'15.3"N, 60°38'27.6"W; 105 m a.s.l.; 24.VII.2014; L. S. Carvalho and M. C. Schneider leg.; CHNUFPI 1979, CHNUFPI 2558 • 2 ♀; same data; CHNUFPI 1990, CHNUFPI 2559 • 1 juv.; same data; CHNUFPI 1994.

Type locality. — Cantá, state of Roraima, Brazil.

Diagnosis. — *Microtityus adriki* n. sp. seems to be most closely related to *Microtityus ambarensis* (Schawaller 1982), *M. biordi* González-Sponga, 1970 and *M. litoralensis* González-Sponga, 2001 from Venezuela, and *M. vanzolinii* Lourenço & Eickstedt, 1983 from Brazil, sharing with them an orthobothriotaxic trichobothrial pattern on the pedipalp femur (11 trichobothria: d_1-d_5, e_1, e_2, and i_1-i_4) (Fig. 3A-D) and the pedipalp patella (13 trichobothria: d_1-d_5, eb_1, eb_2, esb_1, esb_2, *em*, *est*, *et*, and *i*) (Fig. 3E-H). However, *Microtityus adriki* n. sp. and *M. litoralensis* can be readily distinguished from *M. ambarensis*, *M. biordi* and *M. vanzolinii* based on the absence of the trichobothrium *esb* on the pedipalp chela (neobothriotaxic pattern) (Fig. 4A, D). Whereas, *M. ambarensis*, *M. biordi* and *M. vanzolinii* have trichobothrium *esb* on the pedipalp chela (orthobothriotaxic pattern).
On the other hand, *Microtityus adriki* n. sp. can be distinguished from *M. litoralensis* by the presence of trichobothria Eb_3 and *Esb* on the pedipalp chela (Fig. 4A, D) and the position of trichobothrium *db* which is distal to *et* on the pedipalp chela fixed finger (Fig. 4A, B, D, E). Whereas, in *M. litoralensis* trichobothria Eb_3 and *Esb* are absent on the pedipalp chela and the relative position of trichobothrium *db* is proximal to *et* on the pedipalp chela fixed finger (González-Sponga 2001: fig. 10).

Etymology. — Name in apposition is a patronym honoring the Brazilian arachnologist Dr Adriano B. Kury (MNRJ), nicknamed "Adrik", for his contribution to the field of arachnology and especially for his efforts towards reconstruction of the Museu Nacional do Rio de Janeiro.

COI barcode (GenBank accession number: ON856537). —
TCCCGGCAAAATCAAGATATAAACCTCCGGGTGACCAAAAAAC-
CAAAACAAATGTTGATATAAGATAGGATCCCCCCCTCCCGCAG-
GATCAAAAAATCTAGTATTAAAATTCCGGTCTGTCAAAA-
GTATCGTAATAGCCCCAGCAAGAACAGGAAGAGATAAAA-
GCAACAACACAGCTGTAACCAACACAGATCACACAAACAACG-
GAATTCGACTAACCCCTATCCCAGCTCTTCGTATGTTTA-
CAATAGTAGAAATAAAATTAATAGCCCCAAAATAGAGGACGC-
CCCCGCCAGATGAAGGGAAAAAATAGTCAAATCTACAGATC-
CTCCAGAATGAGCCAAAGAAGACGAAAGAGGGGGATACACA-
GTTCACCCTGTTCCAGCCCCCCCCTCCAACGCAGCTGAAGA-
TAAAAGCAAAAAAAAAGCAGGAGGAAGAAGTCAAAATCTTAT-
ATTATTCATACGAGGAAAAGCCATATCAGGAGCCCCAATTAT-
TAACGGAACCAACCAATTCCCAAACCCCCCAATTATAATAG-
GCATAACCATAAAAAAAATCATCACAAAAGCATGAGCAGTAAC-
CACAACATTATAAACCTGATCATCACCAATTAAAGAACCAGC-
CATCCCAATCTCCCCCCGAATCAATAATCTTAAAGACGT

Description

Based on the ♀ holotype (MZSP 76547) and ♂ paratype (MZSP 76548). Total length, ♀, 15.72 mm and ♂, 12.39 mm (see Table 2).

Coloration

Body. General body coloration (in ethanol 70%) (Fig. 1A-D) dark yellow, moderately covered with dark reddish-brown variegated spots.

Carapace. Moderately covered with dark reddish-brown variegated spots; lateral and median eyes surrounded by black spots; posterior area to the median ocular tubercle with a triangular spot.

Chelicerae. Coxa and hand light yellow; hand with dark brown reticulated spots restricted to the anterior margin, rest of the hand immaculate; movable and fixed fingers with dark brown spots on their posterior halves; teeth dark reddish-brown.

Table 2. — Measurements (mm) of *Microtityus* (*Microtityus*) *adriki* n. sp.

		Holotype	Paratypes												
		♀	♂	♀	♀	♂	♀	♀	♂	♂	♀	♀	♂	♀	♀
		MZSP				CHNUFPI				INPA		MNRJ			
Structure	**Measurements**	**76547**	**76548**	**76549**	**76549**	**2558**	**2559**	**1990**	**1979**	**00623**	**00624**	**7685**	**7685**	**7685**	**7685**
Body	Total length	15.72	12.39	17.31	15.84	14.67	18.53	19.47	15.20	12.86	16.35	12.87	13.13	13.82	16.62
Carapace	Length	1.47	1.10	2.26	2.36	1.93	2.13	2.60	2.00	1.86	2.38	1.94	1.95	1.89	2.30
	Anterior width	3.00	2.11	1.35	1.35	1.07	1.33	1.40	1.13	1.10	1.39	1.17	1.17	1.24	1.39
	Posterior width	0.21	0.18	2.66	2.97	2.13	2.87	3.00	2.20	2.11	2.90	2.34	2.25	2.48	2.85
	Eye diameter	0.24	0.18	0.18	0.20	0.17	0.23	0.23	0.20	0.16	0.19	0.15	0.17	0.15	0.20
	Interocular distance	0.26	0.19	0.23	0.22	0.17	0.20	0.23	0.20	0.20	0.22	0.20	0.20	0.20	0.23
	cular diada width	0.51	0.42	0.47	0.50	0.53	0.50	0.53	0.43	0.42	0.51	0.43	0.43	0.44	0.51
Tergite I	Length	0.39	0.19	0.39	0.22	0.40	0.40	0.40	0.33	0.20	0.31	0.20	0.16	0.27	0.36
Tergite II	Length	0.38	0.31	0.54	0.29	0.33	0.47	0.53	0.40	0.26	0.34	0.31	0.26	0.30	0.44
Tergite III	Length	0.43	0.34	0.52	0.39	0.47	0.67	0.67	0.47	0.32	0.46	0.36	0.32	0.40	0.57
Tergite IV	Length	0.56	0.40	0.61	0.43	0.53	0.80	0.73	0.60	0.35	0.55	0.43	0.38	0.48	0.69
Tergite V	Length	0.54	0.48	0.63	0.49	0.67	0.87	0.93	0.67	0.39	0.58	0.46	0.43	0.50	0.74
Tergite VI	Length	0.67	0.56	0.83	0.58	0.73	1.00	1.00	0.73	0.48	0.68	0.51	0.42	0.56	0.94
Tergite VII	Length	1.42	0.98	1.37	1.45	1.33	1.60	1.60	1.20	1.08	1.33	0.96	0.98	1.09	1.26
Mesosoma	Total Length	4.39	3.26	4.89	3.85	4.47	5.80	5.87	4.40	3.08	4.25	3.23	2.95	3.60	5.00
Metasoma I	Length	1.13	0.95	1.42	1.16	1.00	1.33	1.33	1.00	0.91	1.23	0.94	0.92	0.96	1.14
	Width	0.92	0.91	0.96	1.13	0.93	1.20	1.20	0.93	0.92	1.15	0.96	0.98	1.00	1.14
	Height	1.04	0.81	0.87	1.02	0.80	1.00	1.00	0.80	0.83	1.05	0.82	0.86	0.82	1.01
Metasoma II	Length	1.47	1.23	1.61	1.50	1.20	1.60	1.67	1.27	1.19	1.48	1.20	1.19	1.26	1.41
	Width	0.83	0.75	0.90	0.94	0.73	1.00	1.00	0.80	0.78	0.90	0.86	0.81	0.80	0.92
	Height	0.99	0.79	0.82	0.87	0.73	0.93	1.00	0.80	0.77	0.97	0.73	0.82	0.82	0.87
Metasoma III	Length	1.66	1.39	1.75	1.63	1.40	1.80	1.87	1.47	1.32	1.61	1.31	1.35	1.32	1.54
	Width	0.77	0.72	0.83	0.81	0.73	0.87	0.93	0.73	0.74	0.91	0.79	0.77	0.71	0.84
	Height	0.98	0.70	0.81	0.86	0.73	0.93	1.00	0.73	0.73	0.89	0.77	0.84	0.77	0.85
Metasoma IV	Length	1.85	1.41	1.74	1.65	1.47	1.93	2.00	1.60	1.38	1.69	1.35	1.48	1.43	1.58
	Width	0.73	0.66	0.80	0.75	0.67	0.87	0.80	0.73	0.67	0.79	0.77	0.73	0.67	0.84
	Height	0.92	0.66	0.77	0.79	0.67	0.87	0.87	0.80	0.73	0.83	0.72	0.78	0.75	0.79
Metasoma V	Length	2.19	1.79	2.19	2.20	1.80	2.27	2.33	1.87	1.82	2.11	1.68	1.83	1.88	2.10
	Width	0.59	0.59	0.70	0.68	0.60	0.73	0.80	0.60	0.59	0.72	0.68	0.67	0.61	0.71
	Height	0.81	0.60	0.67	0.75	0.67	0.80	0.80	0.67	0.67	0.82	0.69	0.70	0.67	0.79
Metasoma	Length	8.30	6.77	8.71	8.14	6.87	8.93	9.20	7.20	6.62	8.12	6.48	6.77	6.85	7.77
Telson	Vesicle length	0.91	0.80	0.91	0.91	0.93	1.13	1.20	0.93	0.77	0.90	0.73	0.82	0.80	0.89
	Vesicle width	0.57	0.49	0.62	0.56	0.33	0.53	0.53	0.53	0.52	0.57	0.53	0.54	0.51	0.56
	Vesicle height	0.66	0.54	0.62	0.64	0.53	0.67	0.67	0.60	0.56	0.67	0.56	0.59	0.58	0.66
	Aculeus length	0.68	0.50	0.61	0.62	0.53	0.53	0.67	0.60	0.54	0.63	0.47	0.48	0.55	0.62
	Total length	1.56	1.26	1.45	1.49	1.40	1.67	1.80	1.60	1.30	1.60	1.22	1.46	1.48	1.55
Metasoma + Telson	Total length	9.86	8.03	10.16	9.63	8.27	10.60	11.00	8.80	7.92	9.72	7.70	8.23	8.33	9.32
Femur	Length	1.83	1.38	1.64	1.69	1.53	1.87	1.93	1.53	1.29	1.83	1.39	1.49	1.48	1.73
	Width	0.61	0.55	0.63	0.60	0.53	0.73	0.73	0.53	0.54	0.72	0.60	0.52	0.52	0.72
Patella	Length	1.97	1.56	1.84	1.87	1.67	2.13	2.13	1.67	1.53	1.99	1.59	1.58	1.57	1.91
	Width	0.91	0.65	0.82	0.89	0.73	0.93	0.87	0.73	0.68	0.79	0.71	0.69	0.69	0.88
Chela	Length	2.98	2.14	2.71	2.85	1.67	2.93	3.13	2.47	2.27	2.85	2.15	2.44	2.52	2.74
	Width	0.66	0.53	0.69	0.65	0.47	0.67	0.67	0.53	0.58	0.72	0.58	0.57	0.59	0.68
	Height	0.59	0.50	0.60	0.63	0.53	0.73	0.80	0.60	0.50	0.70	0.56	0.52	0.54	0.59
	Length mov. fing.	1.87	1.28	1.74	1.73	1.40	1.80	2.00	1.53	1.45	1.88	1.39	1.54	1.64	1.75
	Length fix. fing.	1.84	1.07	1.44	1.50	1.13	1.47	1.60	1.27	1.39	1.54	1.26	1.51	1.29	1.44
	Length palm	1.13	0.90	1.07	1.20	0.93	1.20	1.20	1.00	0.91	1.12	0.88	0.90	1.21	1.09

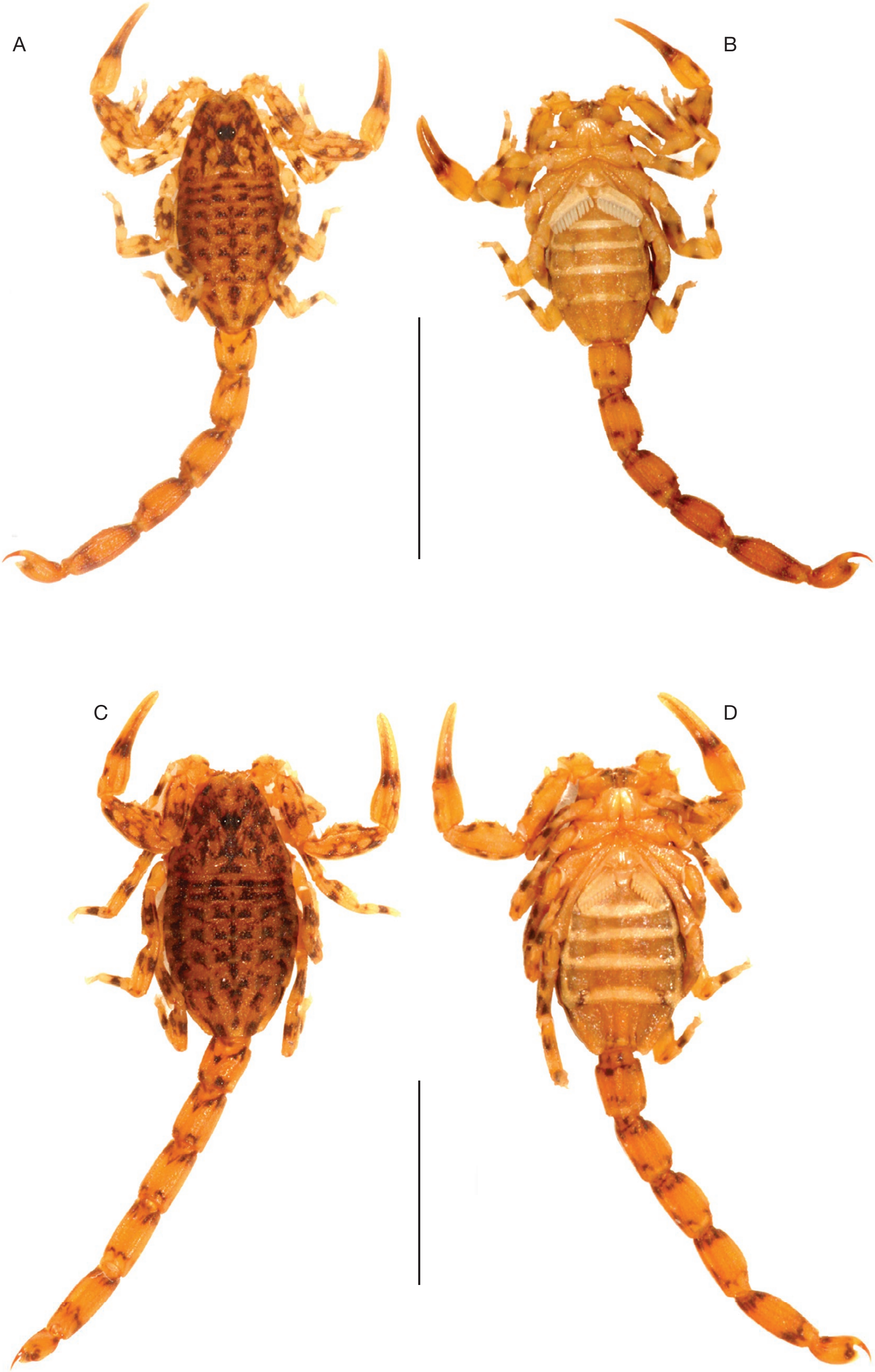

FIG. 1. — *Microtityus* (*Microtityus*) *adriki* n. sp.: **A**, **B**, ♂ paratype (MZSP 76548): dorsal (**A**); ventral (**B**); **C**, **D**, ♀ holotype (MZSP 76547): dorsal (**C**); ventral (**D**). Scale bars: 5 mm.

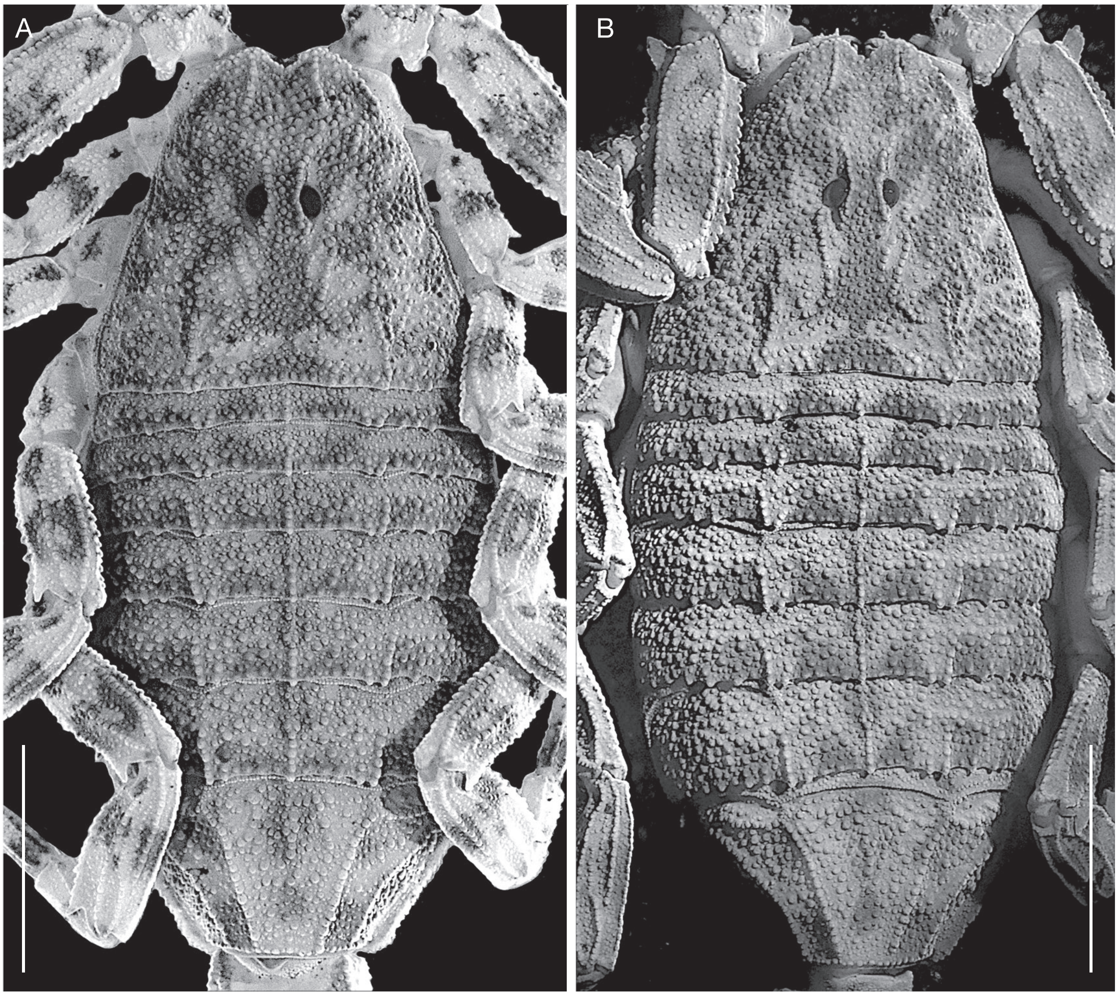

Fig. 2. — *Microtityus* (*Microtityus*) *adriki* n. sp., carapace and tergites sculpturing, dorsal: **A**, ♂ paratype (MZSP 76548); **B**, ♀ holotype (MZSP 76547). Scale bars: A, 2.0 mm; B, 3.0 mm.

Pedipalps. Moderately covered with dark reddish-brown variegated spots and yellow spots; trochanter, femur, patella and chela ventrally yellow; trichobothrial pits yellow.

Legs. All segments light yellow, moderately covered with dark brown variegated spots on their prolateral surfaces.

Coxosternal region. Coxae I-IV, sternum, genital operculum, pectines and basal pectinal piece light yellow; basal pectinal piece with a posterior white area.

Mesosoma. Tergites I-VII and sternites VI-VII dark yellow, moderately and slightly covered with dark reddish-brown variegated spots, respectively; pre-tergites on tergites I-VII with four lateral dark reddish-brown spots; post-tergite on tergites I-VII with six dark reddish-brown spots (four lateral and two submedian); spiracles yellow.

Metasoma. Dark yellow slightly covered with dark reddish-brown variegated spots; DSM intercarinal areas of segments I-IV each with an anterior median arrow-shaped, brown spot, and a distal pair of brown spots; VSM and VM intercarinal areas of segments I-IV each with a pair of proximal and distal brown spots.

Telson. Yellowish, slightly covered with brown spots; subaculear tubercle with brown spots; aculeus dark reddish-brown.

Morphology

Carapace (Fig. 2A, B). Densely covered with fine and coarse granules; anterior margin with a deep median notch; anterior median, superciliary, lateral ocular, central lateral, central median, posterior lateral and posterior median carinae well-marked; anterior marginal, anterior median, median ocular, and posterior marginal furrows well-marked; posterior median, lateral ocular, central lateral and central median furrows shallow; median ocular tubercle well-marked and located on the anterior half of the carapace; median eyes separated by one ocular diameter. Lateral eyes pattern type 4A, with three

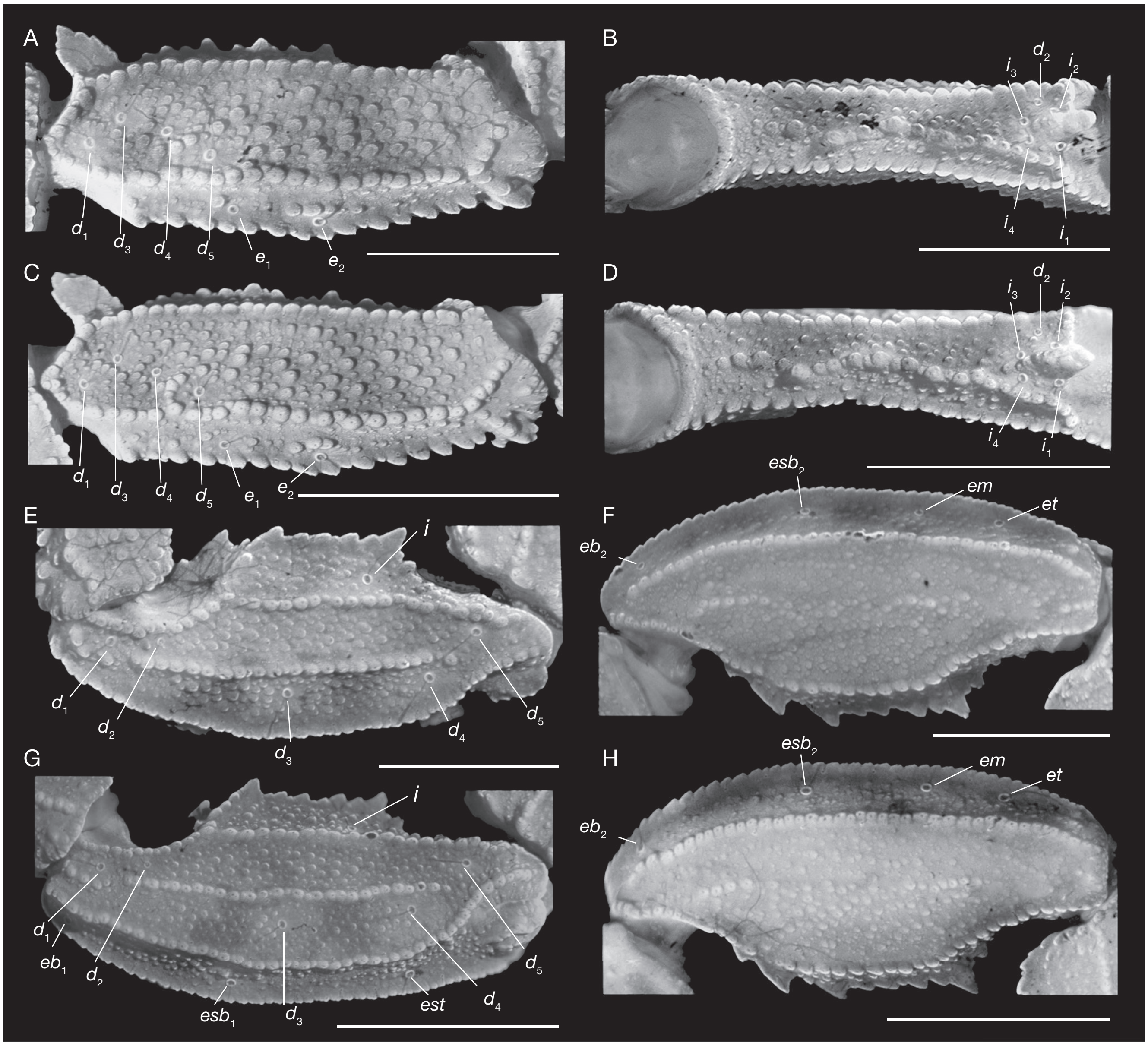

Fig. 3. — *Microtityus* (*Microtityus*) *adriki* n. sp., dextral pedipalp femur and patella sculpturing: **A**-**D**, femur: **A**, **B**, ♂ paratype (MZSP 76548); dorsal (**A**), internal (**B**); **C**, **D**, ♀ holotype (MZSP 76547): dorsal (**C**), internal (**D**); **E**-**H**, patella: **E**, **F**, ♂ paratype (MZSP 76548); dorsal (**E**), ventral (**F**); **G**, **H**, ♀ holotype (MZSP 76547); dorsal (**G**); ventral (**H**). Abbreviations: ***d***, dorsal; ***e***, external; ***eb***, external basal; ***esb***, external sub-basal; ***em***, external median; ***est***, external subterminal; ***et***, external terminal; ***i***, internal. Scale bars: 0.7 mm.

pairs of major ocelli (PLMa, MLMa, and ALMa) and one pair of minor ocelli (ADMi).

Chelicerae. Dentition characteristic of the family Buthidae (Vachon 1963); hand and fingers densely covered with setae on the internal and ventral surfaces.

Pedipalps

Femur (Fig. 3A-D). With five well-marked and complete carinae: VI, IM, DI and DE crenulate; VE serratocrenulate; internal intercarinal area with a conspicuous basal spur of truncate apex projected backwards; intercarinal areas densely covered with fine and coarse granules.

Patella (Fig. 3E-H). With seven carinae well-marked: VI, VE, DI, DM, DE and EM complete and crenulate; IM complete and serratocrenulate, with two spurs one on its base and another one on its apex; intercarinal areas densely covered with coarse granules and few fine granules.

Chela (Tibia) (Fig. 4A-F). Chela no-incrassate. With nine carinae well-marked: VI, VE, D, DS and ES complete and crenulate; DI and DMA complete and serratocrenulate; SA incomplete and crenulate, only present on the anterior third and the distal third of the hand. Pedipalp movable and fixed fingers without lobes (Fig. 4A, D); dorsal surface of movable finger with 11-10 (♀) and 10-10 (♂) oblique rows of denticles.

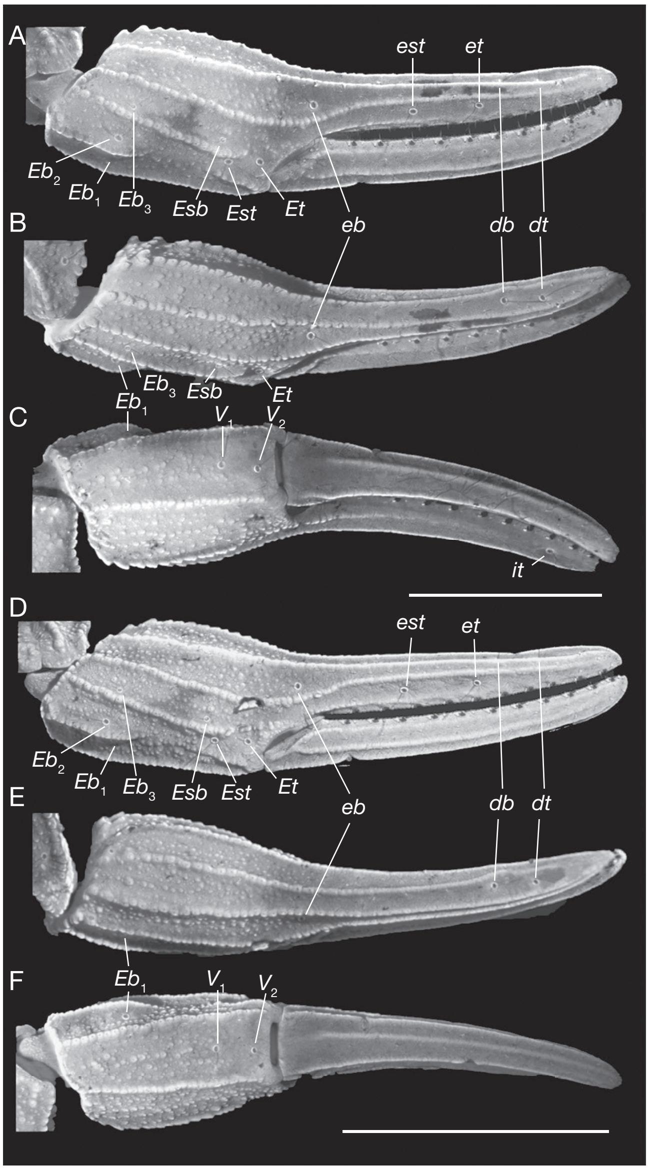

FIG. 4. — *Microtityus* (*Microtityus*) *adriki* n. sp., dextral chela sculpturing; **A**-**C**, ♂ paratype (MZSP 76548): external (**A**), dorsal (**B**), ventral (**C**); **D**-**F**, ♀ holotype (MZSP 76547); external (**D**); dorsal (**E**); ventral (**F**). Abbreviations: ***db***, dorsobasal; ***dt***, dorsoterminal; ***Eb***, ***eb***, external basal; ***Esb***, external sub-basal; ***Est***, ***est***, external subterminal; ***Et***, ***et***, external terminal; ***it***, internal terminal; ***V***, ventral. Scale bars: 1.0 mm.

Trichobothria. Femur with orthobothriotaxic pattern (11 trichobothria: d_1-d_5, e_1, e_2 and i_1-i_4) (Fig. 3A-D), d_2 petite located on the dorsointernal surface, and d_3 located in the dorsomedian region in between DE and DI carinae (α configuration) (Fig. 3A, C); patella with orthobothriotaxic pattern (13 trichobothria: d_1-d_5, eb_1, eb_2, esb_1, esb_2, *em*, *est*, *et* and *i*) (Fig. 3E-H), d_2 petite; chela with neobothriotaxic pattern (14 trichobothria: *db*, *dt*, Eb_1-Eb_3, *Esb*, *Est*, *Et*, *eb*, *est*, *et*, *it*, V_1 and V_2) (Fig. 4A-F), Eb_3 and *Esb* petite, *esb* absent; *db* and *dt* located between the DMA and DS carinae, *db* distal to *est*, V_1 and V_2 unaligned.

Coxosternal region (Fig. 5A, B). Densely covered with coarse granules and few fine granules, except for coxapophyses I-II that are smooth. Sternum with posterior depression, outer ridge, and apical button well-marked. Genital operculum longitudinally divided and composed of two subtriangular plates.

Pectines (Fig. 5A, B). Basal piece with a deep anteromedian notch and not projected posteriorly (♂) (Fig. 5A) or a concave anterior margin and strongly projected posteriorly (♀) (Fig. 5B); posterior margin rounded without glandular region (♂) (Fig. 5A) or truncate and with glandular region (♀) (Fig. 5B); pectinal tooth count: 10-9 (♀) and 11-11 (♂). Intermediate plates, marginal plates and fulcra moderately covered with setae.

Legs. Carinae present; intercarinal areas with few fine granules; claws short and symmetrical.

Mesosoma. Tergites I-VI (Fig. 2A, B) densely covered with coarse and fine granules; pre-tergite well-marked; post-tergites I-VI with single median, paired paramedian lateral and paired median lateral carinae; paramedian lateral and median lateral carinae slightly projected in the posterior margin of the post-tergite; paramedian lateral carinae composed of two to three coarse granules; tergite VII with DSM and DL carinae complete and crenulate, median carina located on the anterior half and crenulate. Sternites (Fig. 5A-D) densely covered with coarse and fine granules; sternites IV-VI each with longitudinal median hyaline suture and a pair of ovate spiracles on the posterior half; spiracles progressively enlarged towards sternite VI; posterior margin of sternite V with a small (♂) (Fig. 5C) or vestigial (♀) subcircular glandular area (Fig. 5D); sternite VI with paired VSM and VL carinae crenulate and occupying the two posterior thirds of the sternite; sternite VII with VSM carinae crenulate and occupying more than two posterior thirds of the sternite, and VL carinae crenulate occupying the anterior half of the sternite.

Hemispermatophore (Fig. 6A-C). Thin and sclerotized; foot narrow and flat; pedal flexure inconspicuous; body occupying two-thirds of the hemispermatophore total length; *pars recta* perpendicular with respect to the body on the basal half and non-perpendicular and spatulate in the distal half (lateral view), with a median diaphanous oval-shaped expansion on the basal half (anterior and posterior views) (Fig. 6A, C); *pars recta* anterior margin with a ridge connecting with the basal lobe base (Fig. 6B); *pars reflexa* with an uncoiled flagellum (Fig. 6A, C). Capsular region (Fig. 6A-C) internal lobe with a rounded tip forming a 80° angle (Fig. 6B); external lobe thin and acute, not overpassing the internal lobe level and with a translucent area between the base of the basal lobe and the base of the internal lobe (Fig. 6C); translucent area basally wide but progressively narrower towards the distal region (Fig. 6C); basal lobe ovate-shaped with an anterior margin straight in lateral view (Fig. 6B) and slightly curved in anterior and posterior views; basal lobe forming a shallow

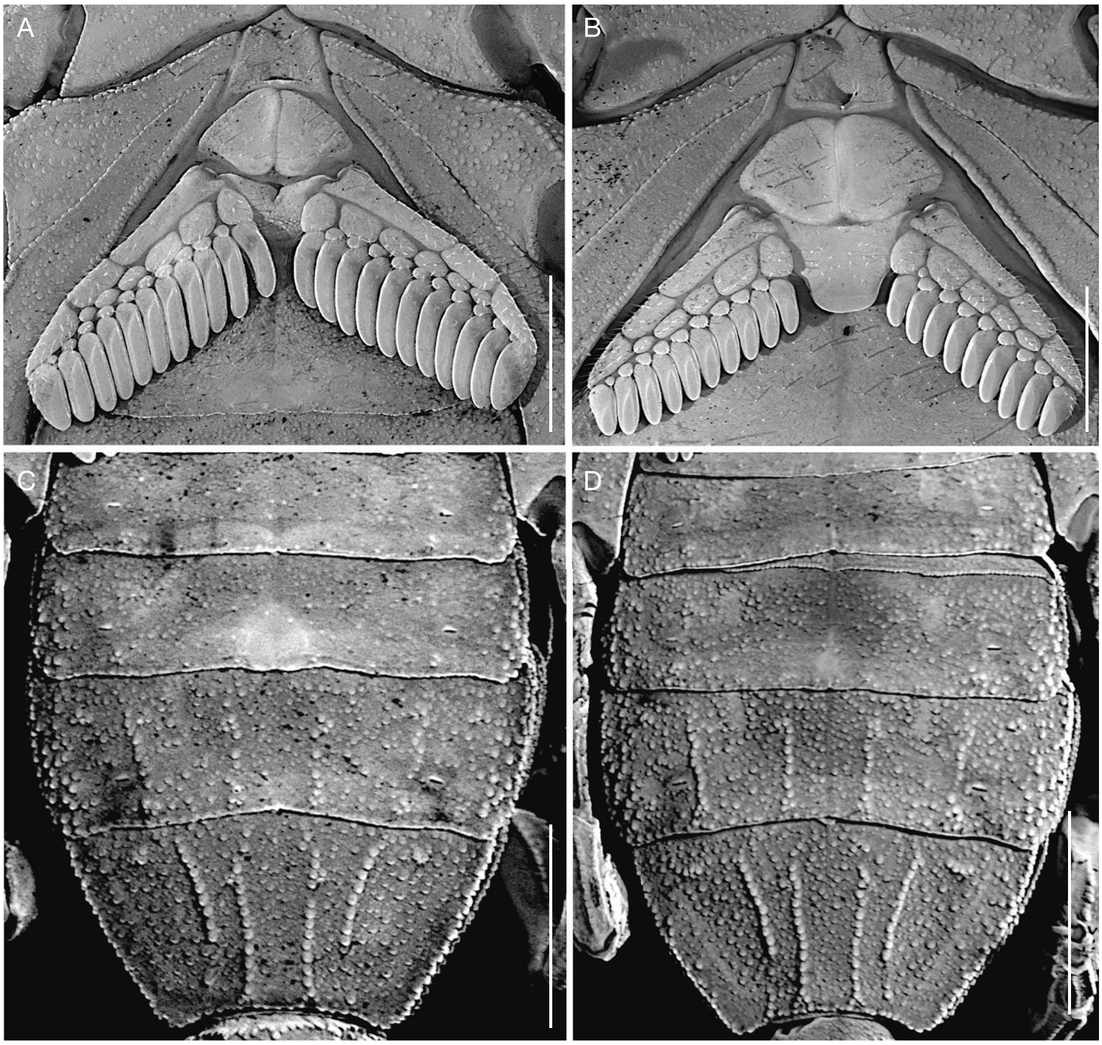

FIG. 5. — *Microtityus* (*Microtityus*) *adriki* n. sp., pectines and sternites sculpturing: **A**, **C**, ♂ paratype (MZSP 76548); pectines (**A**); sternites IV-VII (**C**); **B**, **D**, ♀ holotype (MZSP 76547); pectines (**B**); sternites IV-VII (**D**). Scale bars: A, B, 1.0 mm; C, 1.5 mm; D, 2.5 mm.

U-shaped curve with the body (Fig. 6A, C); basal lobe not elongated with a rounded apex and approximately as long as its basal width in anterior view (Fig. 6A).

Metasoma (Fig. 7A-D). Segments II-V not elongated (length/width ratio: II = ♂, 1.67, ♀, 1.77; III = ♂, 1.93, ♀, 2.16; IV = ♂, 2.16, ♀, 2.53; V = ♂, 3.03, ♀, 3.71); segment V not incrassate. Segments I-II with 10 complete, parallel and crenulate carinae (paired DL, ML, LIM, VL and VSM; DL serratocrenulate on segment II); LIM on segment II composed of coarse granules on the two posterior thirds and irregularly distributed coarse granules on the first anterior third; intercarinal areas densely covered with fine granules and moderately covered with coarse granules. Segments III-IV with eight complete, parallel and crenulate carinae (paired DL, ML, VL and VSM; DL serratocrenulate); intercarinal areas densely covered with fine granules and moderately covered with coarse granules. Segment V with nine complete and crenulate carinae (VM, paired VSM, VL, LIM and ML); lateral and ventral intercarinal areas densely covered with coarse granules and moderately covered with fine granules. Segment II-IV with DL carinae composed of granules that slightly increase in size towards the distal region of each segment, without ending in a conspicuous enlarged granule.

Metasomal macrosetation. Segments I-IV each with two pairs of VSM macrosetae (VSM_1, VSM_3) and two pairs of VL macrosetae (VL_1, VL_2): pair VSM_1 located close to the anterior margin of the segment, and pair VSM_3 close to the posterior margin of the segment; pair VL_1 located close to the anterior margin of the segment and VL_2 on the second posterior third of the segment. Segment V with two pairs of VSM macrosetae (VSM_1, VSM_3), three pairs of VL macrosetae (VL_1, VL_2, VL_3), and one pair of ML macrosetae (ML_1): pair VSM_1 located close to the anterior margin of the segment and pair VSM_3 on the anal arch area; pair VL_1 located close to the anterior margin of the segment; pair VL_2 located on the second posterior third of the segment, and pair VL_3 on the anal arch area; ML_1 located close to the posterior margin of the segment.

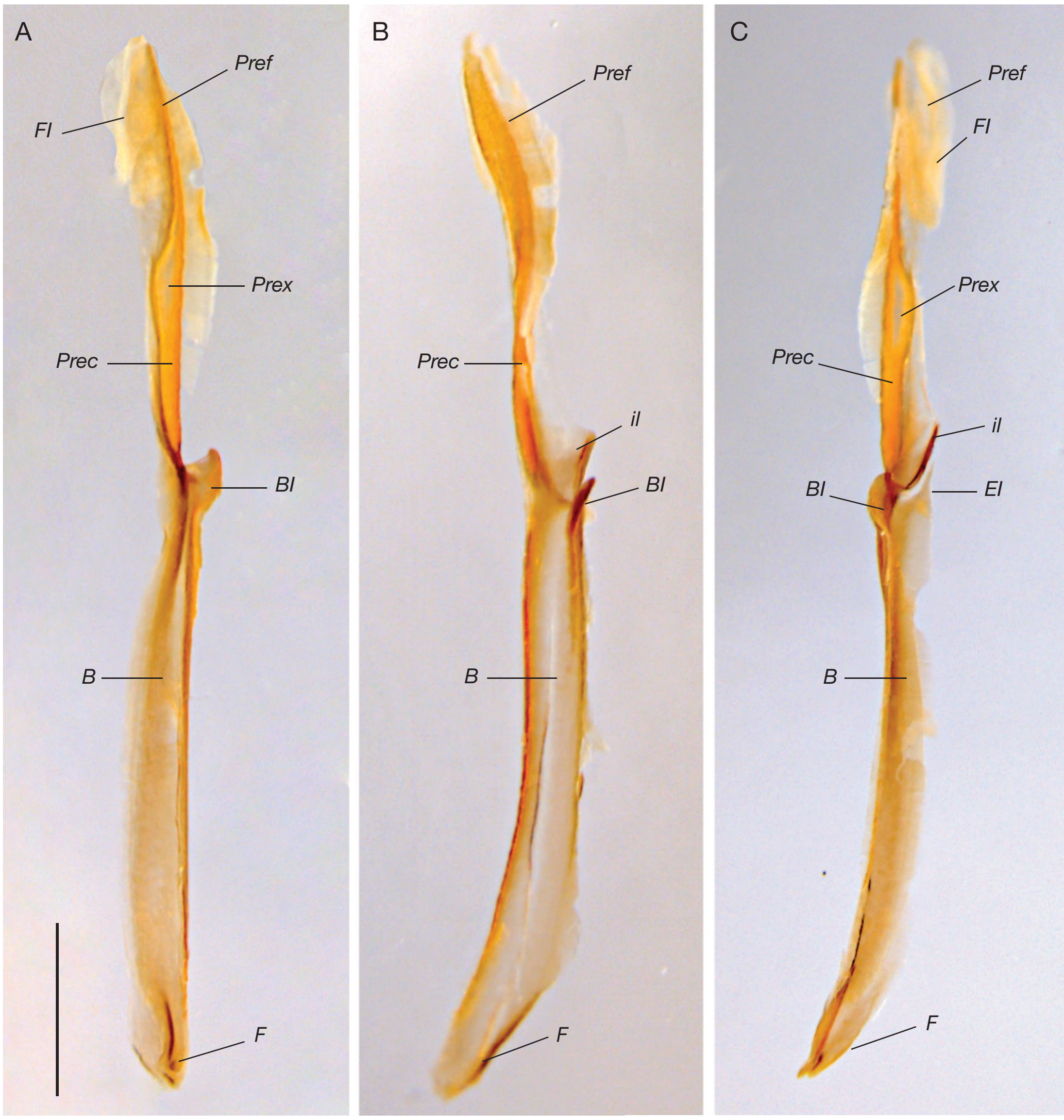

FIG. 6. — *Microtityus* (*Microtityus*) *adriki* n. sp., dextral hemispermatophore, ♂ paratype (CHNUFPI 1979); **A**, posterior view; **B**, lateral view; **C**, anterior view. Abbreviations: ***B***, body; ***Bl***, basal lobe; ***El***, external lobe; ***F***, foot; ***Fl***, flagellum; ***il***, internal lobe; ***Prec***, *pars recta*; ***Pref***, *pars reflexa*; ***Prex***, *pars recta* expansion. Scale bar: 500 µm.

Telson (Fig. 8A, B). Vesicle slightly elongated and suboval (length/height ratio: ♀, 1.38, ♂, 1.48) with a smooth dorsal surface and a shallow lateral longitudinal furrow on each lateral surface; with 11 crenulate carinae (single VM and paired VSM, VL, ML, DL and DSM): VM, VSM, VL, VSL and ML slightly marked; VSM reaching the base of the subaculear tubercle; VL ending at the same level of the VSM; ML and DL occupying the two anterior thirds of the vesicle. Subaculear tubercle large, pyramidal, crest-like, and with a rounded apex, with the apex pointing to the middle section of the aculeus; dorsal margin of the subaculear tubercle with a pair of small and rounded granules; aculeus slightly curved, shorter than vesicle and with a ventral groove.

Variability. *Total length* (*including telson*): ♂, 12.39-15.20 mm (n = 5; mean= 13.65; StDv = 1.22), ♀, 15.72-19.47 mm (n = 9; mean = 16.28; StDv = 2.08). *Pectinal tooth counts*: ♂, 10-11 (n = 10; mode = 10), ♀, 9-11 (n = 20; mode = 10). *Number of movable finger oblique rows of denticles*: ♂, 10-11 (n = 10; mode = 11), ♀, 10-11 (n = 19; mode= 11).

Natural History. All known specimens of *Microtityus adriki* n. sp. were collected using UV flashlights at night on rocky outcrops and in the leaf litter inside the forest. The color pattern of this species camouflages it within the leaf litter (Fig. 9A, B) and rocks of the area. During capture, they compressed their body, legs, and metasoma against the rocks, making it difficult to collect them with tweezers.

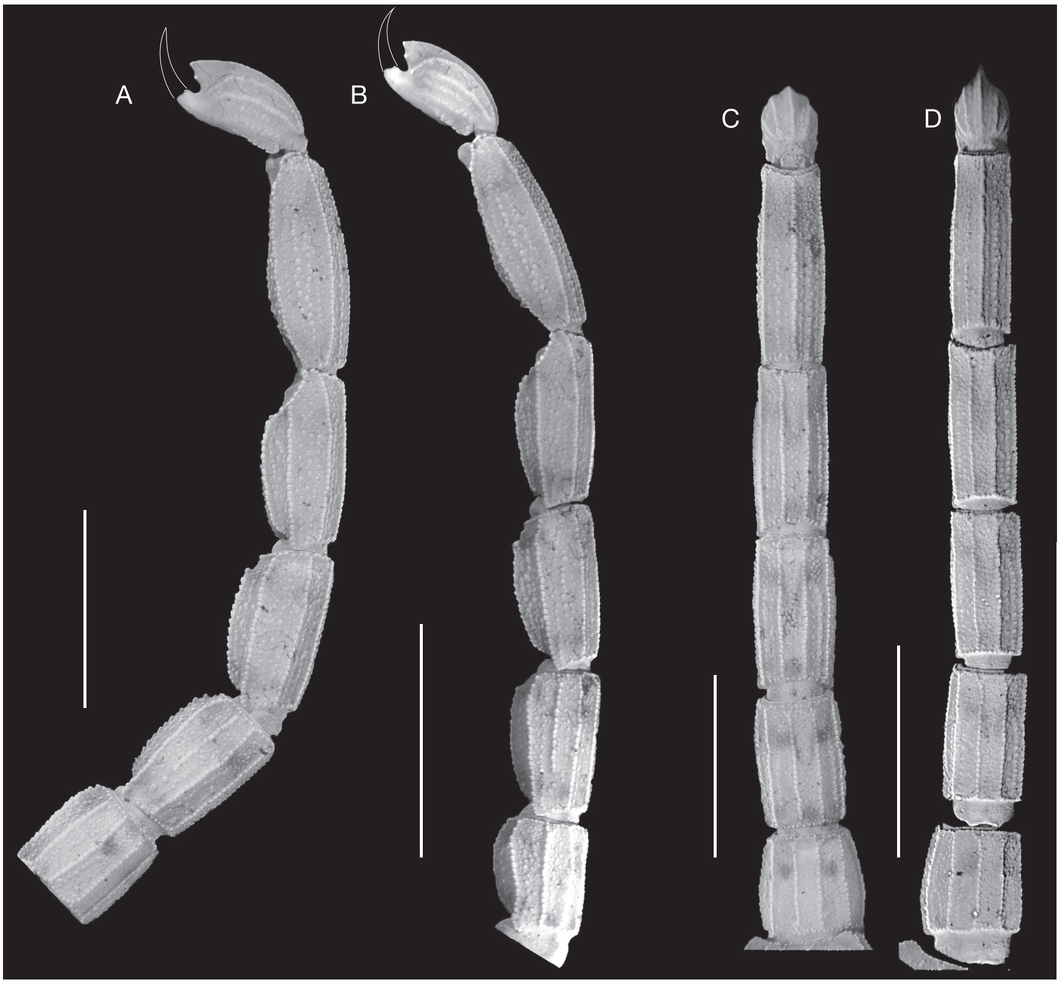

Fig. 7. — *Microtityus* (*Microtityus*) *adriki* n. sp., metasomal segments I-V and telson: **A**, **C**: ♂ paratype (MZSP 76548); lateral (**A**); ventral (**C**); **B**, **D**, ♀ holotype (MZSP 76547); lateral (**B**); ventral (**D**). Scale bars: 2.0 mm.

Under laboratory conditions, they remain motionless when touched, resembling thanatosis.

Distribution

Microtityus adriki n. sp. is currently known from two closely located (< 5 km) sampling sites in Cantá, state of Roraima, northern Brazil (Fig. 10A).

Potential distribution of *Microtityus*

The Principal Component Analysis (PCA), based on 21 climatic variables (Table 3), revealed that the two most important principal components (PCs) explained 63.5% of the variation (Table 4). The PCA used to explore the environmental niche occupied by *Microtityus*, after sampling 100 random points within a 10 km buffer surrounding each locality record, evidenced that only five axes corresponded to a higher than expected by chance proportion of variance of the environmental heterogeneity (Table 4). The most important variables contributing to the first PC axis were related to temperature (e.g. annual mean temperature, mean temperature of coldest quarter, mean temperature of warmest quarter, max temperature of warmest month, mean

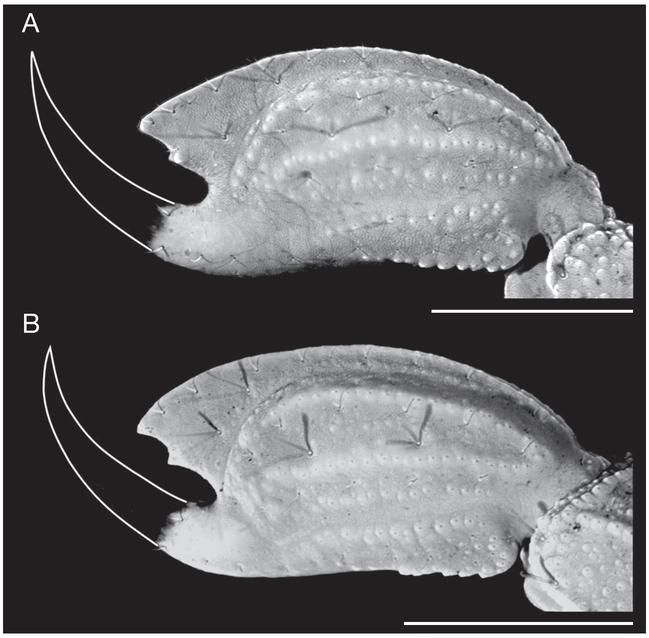

Fig. 8. — *Microtityus* (*Microtityus*) *adriki* n. sp., telson sculpturing, lateral; **A**, ♂ paratype (MZSP 76548); **B**, ♀ holotype (MZSP 76547). Scale bars: 0.5 mm.

Table 3. — Environmental predictors used in the present study.

Variables	Source
Annual mean temperature	WorldClim 2
Annual precipitation	WorldClim 2
Isothermality	WorldClim 2
Max temperature of warmest month	WorldClim 2
Mean diurnal range	WorldClim 2
Mean temperature of coldest quarter	WorldClim 2
Mean temperature of driest quarter	WorldClim 2
Mean temperature of warmest quarter	WorldClim 2
Mean temperature of wettest quarter	WorldClim 2
Min temperature of coldest month	WorldClim 2
Precipitation of coldest quarter	WorldClim 2
Precipitation of driest month	WorldClim 2
Precipitation of driest quarter	WorldClim 2
Precipitation of warmest quarter	WorldClim 2
Precipitation of wettest month	WorldClim 2
Precipitation of wettest quarter	WorldClim 2
Precipitation seasonality	WorldClim 2
Temperature annual range	WorldClim 2
Temperature seasonality	WorldClim 2
Tree canopy height	Simard *et al.* (2011)
Tree density	Crowther *et al.* (2015)

temperature of wettest quarter, mean temperature of the driest quarter, min temperature of coldest month) (Table 5). Conversely, for the second PC axis, the environmental variables related to precipitation played a more significant role (e.g. annual precipitation, precipitation of driest quarter, precipitation of driest month, precipitation of coldest quarter, precipitation of wettest quarter and precipitation of wettest month) (Table 5). The ordination of the random points surrounding each *Microtityus* record evidenced that the environmental niches of *Microtityus adriki* n. sp. and *Microtityus vanzolinii* are similar to those of other *Microtityus* species, primarily in terms of temperature (i.e., see PC1 in Figure 11). However, the environmental niche of *M. vanzolinii* significantly differs that of other *Microtityus* species, especially when considering precipitation (i.e., see PC2 in Figure 11). Furthermore, when considering precipitation (i.e., see PC2 in Figure 11), the environmental niche of *M. adriki* n. sp. exhibits low similarity with non-Brazilian *Microtityus* species, as it falls outside their confidence intervals (see ellipses in Figure 11).

Table 4. — Summary of the significant principal components (**PC**) for the environmental layers used to explore the environmental niche occupied by *Microtityus* Kjellesvig-Waering, 1966 species. The used PCs are those which the proportion of variance was higher than expected by chance (i.e., > 4.76%).

Parameter	PC1	PC2	PC3	PC4	PC5	PC6	PC7
Standard deviation	2.74	2.42	1.67	1.22	1.16	0.89	0.8
Proportion of variance (%)	35.70	27.80	13.20	7.10	6.40	3.80	3.00
Cumulative proportion (%)	35.70	63.50	76.70	83.80	90.20	94.00	97.00

Table 6. — Summary of the significant principal components (**PC**) for the environmental layers used as explanatory variables in the species distribution modeling (SDM) of *Microtityus* Kjellesvig-Waering, 1966 species. The used PCs are those which the proportion of variance was higher than expected by chance (i.e., > 4.76%).

Parameter	PC1	PC2	PC3	PC4	PC5	PC6	PC7	PC8	PC9
Standard deviation	3.07	1.99	1.48	1.09	0.99	0.91	0.86	0.7	0.61
Proportion of variance (%)	45	19	10	6	5	4	3	2	2
Cumulative proportion (%)	45	64	74	80	85	89	92	94	96

Table 5. — Eigenvectors of covariance factor of the principal components (**PC**) for the environmental layers used to explain the distribution of *Microtityus* Kjellesvig-Waering, 1966 species. The used PCs are those which the proportion of variance was higher than expected by chance (i.e., > 4.76%). Variables are sorted in order of importance for the first principal component.

Variables	PC1	PC2	PC3	PC4	PC5	PC6	PC7
Annual mean temperature	0.36	0.07	0.00	–0.04	0.03	–0.11	–0.01
Mean temperature of coldest quarter	0.35	0.09	0.10	–0.01	0.00	–0.07	–0.04
Mean temperature of warmest quarter	0.35	0.05	–0.11	–0.06	0.07	–0.15	0.04
Max temperature of warmest month	0.35	0.00	–0.01	–0.18	0.00	–0.19	0.12
Mean temperature of wettest quarter	0.35	0.02	–0.08	–0.08	0.03	–0.23	–0.13
Mean temperature of driest quarter	0.34	0.10	0.11	0.01	0.01	–0.02	0.03
Min temperature of coldest month	0.34	0.15	0.03	0.09	0.08	–0.02	–0.07
Precipitation seasonality	0.05	–0.22	0.26	–0.28	0.50	0.12	–0.02
Precipitation of coldest quarter	0.04	0.33	0.14	–0.10	0.02	0.29	0.49
Isothermality	0.03	0.05	0.54	–0.05	–0.30	0.02	–0.22
Precipitation of driest month	–0.05	0.36	–0.14	0.02	–0.31	–0.14	0.12
Temperature seasonality	–0.05	–0.10	–0.53	–0.13	0.17	–0.17	0.21
Mean diurnal range	–0.05	–0.20	0.32	–0.41	–0.36	–0.20	0.14
Precipitation of driest quarter	–0.05	0.37	–0.12	0.04	–0.30	–0.10	0.13
Temperature annual range	–0.09	–0.27	–0.07	–0.47	–0.15	–0.27	0.32
Precipitation of wettest quarter	–0.10	0.33	0.11	–0.30	0.24	0.07	0.05
Tree density	–0.11	0.04	0.27	0.37	0.28	–0.54	0.31
Precipitation of wettest month	–0.11	0.32	0.05	–0.27	0.32	0.11	0.05
Annual precipitation	–0.12	0.38	–0.02	–0.17	0.02	–0.06	–0.07
Precipitation of warmest quarter	–0.18	0.20	–0.11	–0.28	0.07	–0.34	–0.61
Tree canopy height	–0.22	0.08	0.23	0.20	0.18	–0.42	0.05

TABLE 7. — Pearson correlation coefficients between the principal components (**PC**) and the environmental layers used as predictors for the species distribution modeling (SDM) for *Microtityus* Kjellesvig-Waering, 1966 representatives. The used PCs are those which the proportion of variance was higher than expected by chance (i.e., > 4.76%). Variables are sorted in order of importance for the first principal component.

Variables	PC1	PC2	PC3	PC4	PC5	PC6	PC7	PC8	PC9
Annual precipitation	0.92	0.18	0.17	–0.25	0.00	–0.10	–0.09	–0.02	–0.02
Precipitation of wettest quarter	0.85	0.00	–0.11	–0.43	0.10	–0.18	–0.15	–0.06	0.01
Precipitation of wettest month	0.83	0.00	–0.13	–0.44	0.10	–0.19	–0.16	–0.07	0.05
Precipitation of coldest quarter	0.71	0.01	0.01	–0.42	–0.14	–0.27	0.35	0.18	–0.04
Precipitation of driest quarter	0.68	0.40	0.55	0.05	–0.14	0.04	0.01	0.17	0.00
Precipitation of driest month	0.64	0.40	0.57	0.08	–0.15	0.06	0.00	0.20	–0.01
Tree canopy height	0.63	0.29	0.05	0.07	0.44	0.08	0.20	–0.28	–0.40
Precipitation of warmest quarter	0.48	0.41	0.43	0.05	0.10	0.14	–0.57	–0.11	0.05
Tree density	0.42	0.27	0.05	0.17	0.75	0.02	0.20	0.19	0.29
Isothermality	0.35	0.13	–0.17	0.06	–0.05	0.10	–0.01	0.11	–0.05
Mean temperature of coldest quarter	0.09	–0.05	–0.03	0.02	0.00	0.02	0.00	0.01	0.00
Mean temperature of driest quarter	0.08	–0.05	–0.02	0.01	0.00	0.01	0.00	0.01	0.00
Annual mean temperature	0.06	–0.05	0.00	0.01	0.00	0.01	0.00	0.00	0.00
Mean temperature of wettest quarter	0.03	–0.06	0.02	0.01	0.00	0.01	0.00	0.00	0.00
Mean temperature of warmest quarter	0.02	–0.06	0.02	0.00	0.00	0.00	0.00	0.00	0.00
Max temperature of warmest month	0.00	–0.07	0.02	–0.01	0.01	0.00	0.00	0.01	–0.01
Mean diurnal range	–0.04	0.00	0.01	–0.01	0.01	0.00	–0.01	0.02	–0.01
Temperature annual range	–0.11	–0.02	0.05	–0.02	0.02	–0.01	0.00	0.01	–0.01
Min temperature of coldest month	–0.19	0.13	0.05	–0.42	–0.03	0.51	0.13	–0.05	0.06
Precipitation seasonality	–0.54	–0.37	–0.53	–0.24	0.22	0.03	–0.27	0.13	0.04
Temperature seasonality	–0.77	–0.12	0.55	–0.13	0.04	–0.12	0.09	–0.07	0.07

TABLE 8. — Estimates of relative contributions of the predictors (described in Tables 6, 7) to the MaxEnt model. Variables are sorted in order of percent contribution.

Variables	Contribution (%)	Permutation importance (%)
PC4	62.10	55.90
PC1	19.40	28.80
PC5	11.00	7.60
PC3	5.90	7.00
PC2	1.50	0.80

Apart from different environmental conditions, the distribution of the genus *Microtityus* is notably disjunct, with species known to exist in both the Antillean and Brazilian biogeographic subregions (e.g., Morrone 2017). The northernmost record in Brazil (i.e., the type locality of *M. adriki* n. sp.) is separated by approximately 900 km from the southernmost record in Colombia (Fig. 10A). By modeling the environmental suitability for the genus, we were able to explore areas with a high potential for discovering new populations of *Microtityus*. For this analysis, five principal components of the spatial PCA of the 21 environmental variables were used (Tables 6; 7). The MaxEnt modeling received a higher percent contribution and permutation importance from PC4 and PC1, which encompassed 81.5% of the model (Table 8). These axes were strongly associated with environmental variables related to precipitation (Table 7).

The species distribution modeling (Fig. 10B) revealed the existence of highly suitable environments for *Microtityus*, in the Antillean subregion (Cuban and Hispaniola provinces; e.g. Cuba, Dominican Republic) and in the Pacific dominion (Guajira and Venezuelan provinces; e.g. Colombia, Venezuela) where there are numerous records of *Microtityus*. Additionally, several locations with no records of *Microtityus* were recovered as highly suitable environments, including sites in the Mesoamerican dominion (e.g., Yucatán Peninsula, in Mexico; and Mosquito province in the Coast of Honduras), Antillean subregion (Jamaica province), Pacific dominion (Cauca, Guajira and Magdalena provinces; e.g. South of Ecuador, Cauca river valley in Colombia, Gulf of Venezuela, Northeast Colombia and south of the Magdalena river valley in Colombia), and in the South Brazilian dominion (Ucayali province; e.g., Amazonian slopes of Ecuadorian Andes). Strikingly, the model does not indicate high suitability in the Sabana province (e.g., Center of Venezuela and Colombian Orinoquia), where no *Microtityus* has been recorded but it is located in between Brazilian and non-Brazilians *Microtityus* records; nor in the Roraima (state of Roraima) and Imerí (state of Amazonas) provinces, where *M. adriki* n. sp. and *M. vanzolini* are found, respectively (Fig. 10B).

DISCUSSION

ON THE MALE HEMISPERMATOPHORE OF *MICROTITYUS*

The male hemispermatophore exhibits extreme morphological stasis in some genera and holds species level characters in others (Monod *et al.* 2017). Notwithstanding, this structure is still unknown for most buthid species of the Americas. In the Neotropical region, a handful of publications have explored the morphology of this structure and contributed to filling this knowledge gap. Some occasional contributions (Bürcherl 1956; Matthiesen 1968, 1976; Lenarducci *et al.* 2005; Prendini *et al.* 2009; Teruel & Armas 2012; Santos *et al.* 2014; Kovařík *et al.* 2015, 2016; Ojanguren-Affilastro *et al.* 2017; Miranda & Armas 2020; Moreno-González *et al.* 2022) as well as some more comprehensive revisions of local

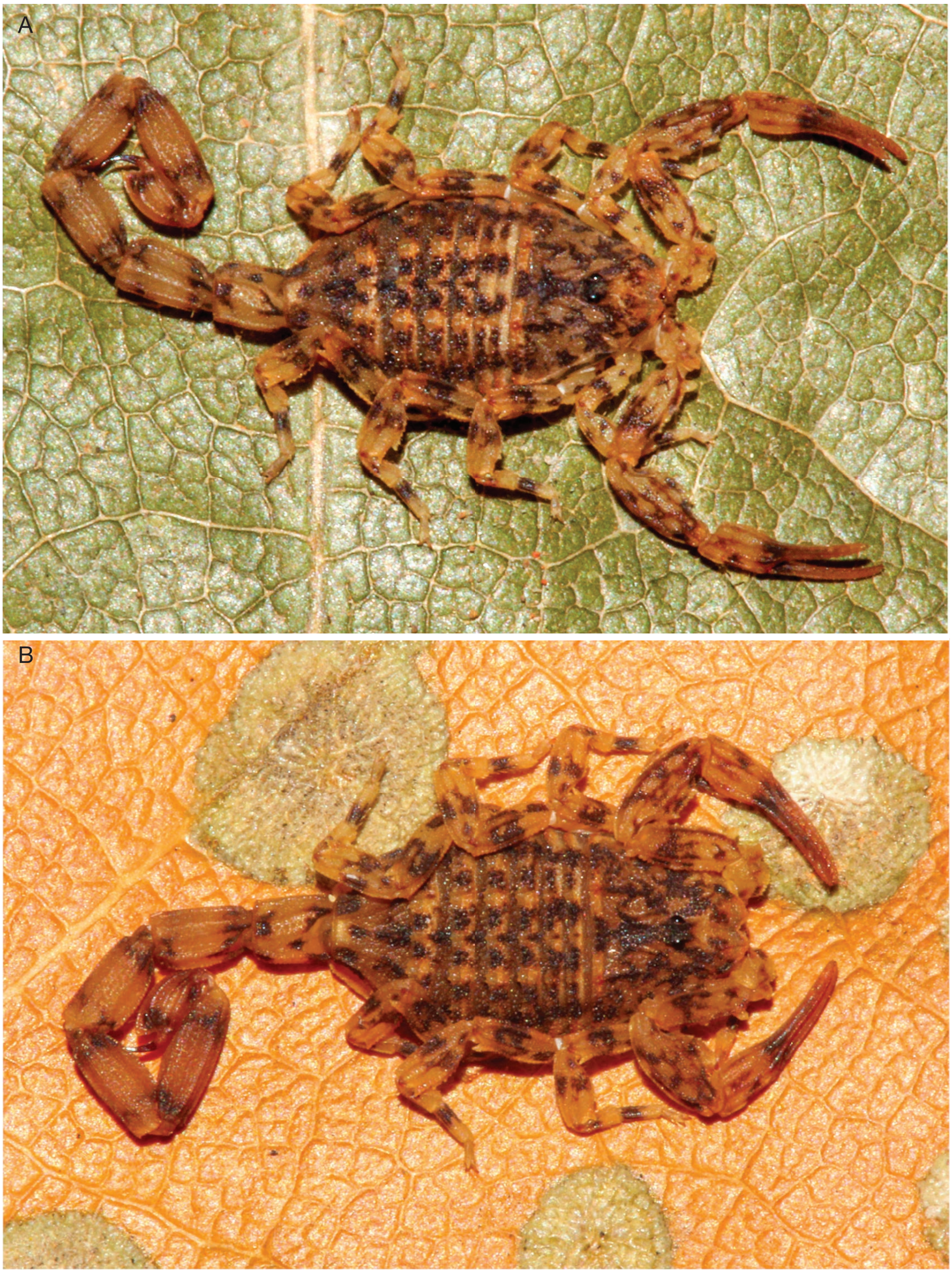

Fig. 9. — *Microtityus* (*Microtityus*) *adriki* n. sp., live habitus: **A**, **B**, females, on leaf litter. Photos: Rogério Bertani.

faunas, species groups, or genera (Francke & Stockwell 1987; Stockwell 1989; Ojanguren-Affilastro 2005; Botero-Trujillo & Flórez 2011; Esposito *et al.* 2017; Moreno-González *et al.* 2019) have included iconography and full descriptions of the male hemispermatophore. However, its morphology is still unknown for a number of Neotropical genera, such as *Microtityus*.

Herein, we describe the morphology of the hemispermatophore of the genus *Microtityus* and detect some remarkable character states. For example, the presence of: 1) a diaphanous oval-shaped expansion in the proximal half of the *pars recta*, in anterior and posterior views (Fig. 6A, C); 2) a ridge connecting the anterior margin of the *pars recta* with the basal lobe base, in lateral view (Fig. 6B); and 3) a *pars reflexa* perpendicular to

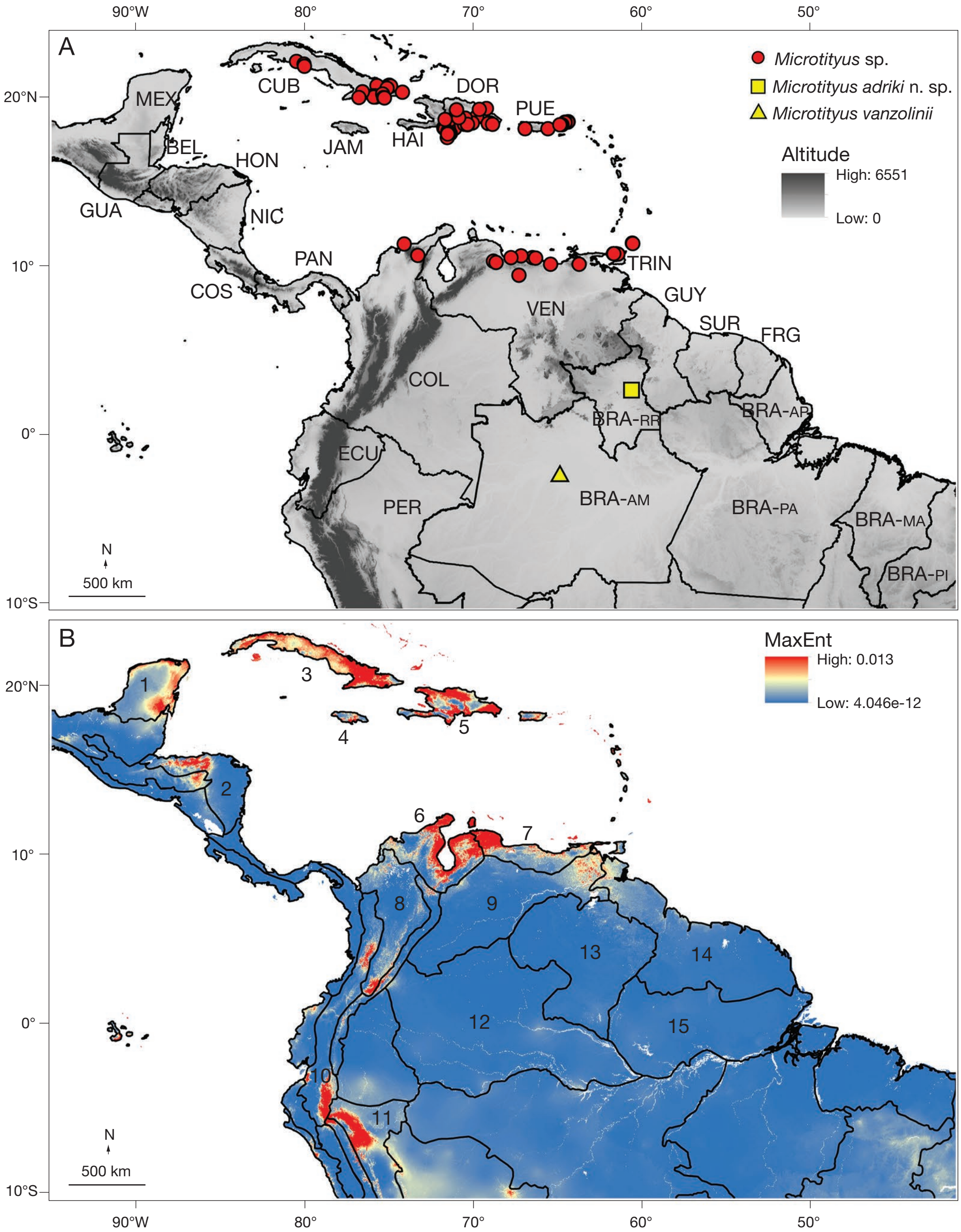

Fig. 10. — Geographical distribution (**A**) and environmental suitability (**B**) of *Microtityus* Kjellesvig-Waering, 1966 species, including *Microtityus adriki* n. sp. (**yellow square**), *Microtityus vanzolinii* Lourenço & Eickstedt 1983 (**yellow triangle**) and other species (**red circles**). The biogeographic regionalisation is depicted in **B**, with numbered regions cited in text. Provinces: **1**, Yucatán Peninsula; **2**, Mosquito; **3**, Cuban; **4**, Jamaica; **5**, Hispaniola; **6**, Guajira; **7**, Venezuelan; **8**, Magdalena; **9**, Sabana; **10**, Cauca; **11**, Ucayali; **12**, Imerí; **13**, Guianan; **14**, Guianan Lowlands, and **15**, Roraima. Abbreviations: **AM**, state of Amazonas; **AP**, state of Amapá; **BEL**, Belize; **BRA**, Brazil; **COL**, Colombia; **COS**, Costa Rica; **CUB**, Cuba; **DOR**, Dominican Republic; **ECU**, Ecuador; **FRG**, French Guiana; **GUA**, Guatemala; **GUY**, Guyana; **HAI**, Haiti; **JAM**, Jamaica; **MA**, state of Maranhão; **MEX**, Mexico; **NIC**, Nicaragua; **PA**, state of Pará; **PAN**, Panama; **PER**, Peru; **PI**, state of Piauí; **PUE**, Puerto Rico; **RR**, state of Roraima; **SUR**, Suriname; **TRIN**, Trinidad and Tobago; **VEN**, Venezuela.

the body on the basal half and non-perpendicular and spatulate in the distal half, in lateral view (Fig. 6B). All these characters have not been recorded in any other Neotropical genera. On the other hand, the capsular region of *Microtityus adriki* n. sp. has three lobes (basal, external, and internal) (Fig. 6C) and genera such as *Ananteris* Thorell, 1891 (e.g. Ojanguren-Affilastro 2005: fig. 28), *Chaneke* Francke, Teruel & Santibáñez López, 2014 (Kovařík *et al.* 2016: figs 33-37), *Heteroctenus* Pocock, 1893 (Esposito *et al.* 2017: fig. 23A-N), *Ischnotelson* Esposito *et al.* 2017 (Esposito *et al.* 2017: fig. 23O-R), *Jaguajir* Esposito *et al.* 2017 (Esposito *et al.* 2017: figs 23S-V, 24A-H), *Physoctonus* Mello-Leitão, 1934 (Esposito *et al.* 2017: fig. 24S-U), *Rhopalurus* Thorell, 1876 (Esposito *et al.* 2017: fig. 24I-R), *Tityus* C.L. Koch, 1836 (e.g. Ojanguren-Affilastro 2005: figs 43, 85,

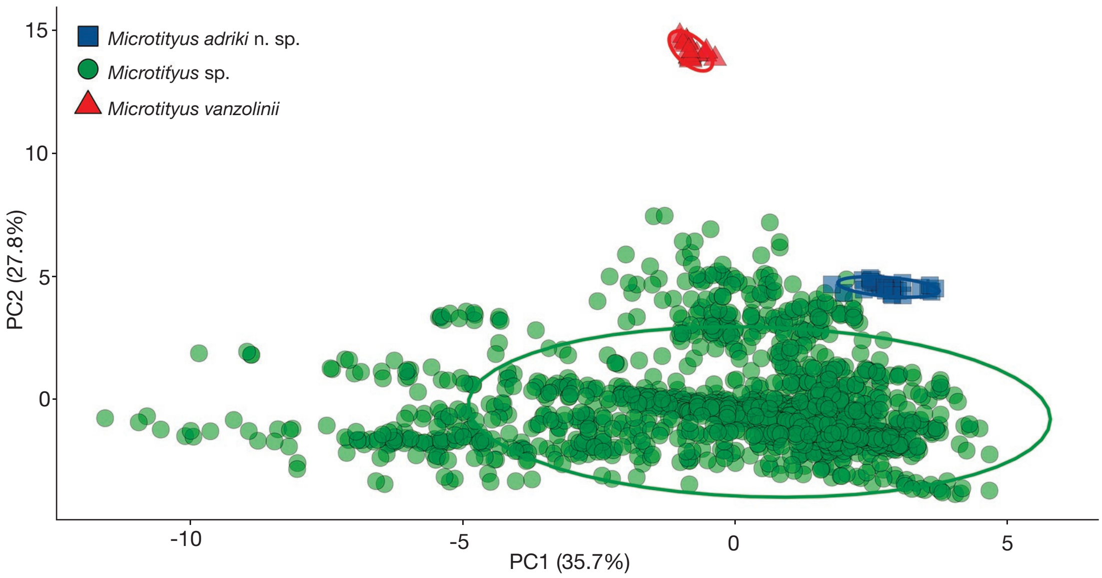

Fig. 11. — Principal component analysis of the environmental conditions for 100 random points within a 10 km buffer surrounding each point of occurrence of *Microtityus* (*Microtityus*) *adriki* n. sp. (**blue squares**), *Microtityus* (*Microtityus*) *vanzolinii* Lourenço & Eickstedt 1983 (**red triangles**), and other *Microtityus* species (**green circles**). The ellipses encompass the values within a multivariate t-distribution (i.e., confidence intervals). Full colors in icons represents an overplotting of 100 points.

94; Kovařík *et al.* 2015: figs 138-141; Ojanguren-Affilastro *et al.* 2017: fig. 6B), and *Zabius* Thorell, 1893 (e.g. Ojanguren-Affilastro 2005: figs 117, 122) also share this character state. Additional surveys on the hemispermatophore morphology of other *Microtityus* species are required to test its potential usefulness for species recognition.

Notes on the biogeography and distribution of *Microtityus*

Microtityus species are distributed in the Antillean subregion, the Pacific and Boreal Brazilian dominions of the Brazilian subregion in the Neotropics (*sensu* Morrone 2017). Within the Pacific dominion, *Microtityus* species are restricted to the Guajira, Venezuelan, and Trinidad biogeographical provinces (Fig. 10A). The two Brazilian species occur in the Imerí (*M. vanzolinii*) and Roraima (*M. adriki* n. sp.) provinces, in the Boreal Brazilian dominion, both known from localities separated from each other by *c.* 700 km, south of the Guiana shield. To date, there is no record of any *Microtityus* species in the Sabana (Antillean subregion), Guianan or Guianan Lowland (Brazilian subregion) provinces, resulting in a disjunct distribution of the genus. Currently, no other scorpion genus exhibits a similar distribution pattern. For instance, a similar pattern was described for *Rhopalurus* Thorell, 1876, which was later split into five different genera after a systematic revision (Esposito *et al.* 2017, 2018).

One hypothesis that could explain the known distribution of *Microtityus* is sampling bias. In fact, both Brazilian species occur in poorly sampled areas (e.g., Oliveira *et al.* 2016, 2017), which are likely to reveal new species or records if sampling increases. This pattern is also observed in most areas without records of *Microtityus* in northern South America (see Hughes *et al.* 2021). However, there have been taxonomic contributions focusing on conspicuous scorpion genera found in some of these areas (e.g. González-Sponga 2009; Lourenço & Duhem 2009, 2010; Lourenço 2016, 2017; Esposito *et al.* 2017, 2018; Ythier 2019; Moreno-González *et al.* 2019). These contributions suggest that the scorpion fauna has not been entirely neglected. On the contrary, our knowledge of scorpions in northern South America has significantly improved in the last decade. The absence of species and records of *Microtityus* is probably explained by biogeographic factors in addition to sampling bias.

For Centruroidinae Kraus, 1955 scorpions, multiple dispersal events occurred across their lineages. Initially, they dispersed within South America during the middle Eocene, followed by one genus dispersing to the Greater Antilles during the Late Eocene/Early Oligocene. Multiple dispersal events of another genus, including movements between Central America, North America, South America, and the recolonisation of the Greater Antilles, during the Miocene (Esposito & Prendini 2019; Crews & Esposito 2020). It is probable that *Microtityus* followed a similar biogeographic history to some extent. The distribution of the Brazilian species was likely influenced by the sea level fluctuations and marine incursions of the Miocene (see Webb 1995; Hoorn *et al.* 1995; Lovejoy *et al.* 1998). However, the absence of phylogenetic hypotheses that include *Microtityus* representatives hampers our understanding of the biogeography of this genus, including its origins, the timing of its diversification, and the direction of its dispersal. These intriguing questions remain to be answered in future studies.

Acknowledgements

This work was partially supported by the Fundação de Amparo à Pesquisa do Estado de São Paulo (FAPESP) (under Grant 2015/18376-2 to JAMG; grant 2011/21643-1 to Marielle Cristina Schneider, and grant FAPESP 2015/19976-3 to RB) and the Conselho Nacional de Desenvolvimento Científico e Tecnológico (CNPq; grant #407288/2013-9 to Adalberto José dos Santos). We thank Francisco Felipe Xavier, Marielle Cristina Schneider and Marlus Queiroz de Almeida for aiding in field work in Roraima. We are grateful to Ricardo Pinto-da-Rocha (IB-USP) for his support and for providing lab facilities to perform the DNA sequencing and the species imaging. Finally, we are grateful to the two anonymous reviewers for their useful comments and suggestions that allowed us to improve this manuscript. This publication is registered in compliance to Brazilian regulations at the Sistema Nacional de Gestão do Patrimônio Genético e do Conhecimento Tradicional Associado (SISGen; #A421144).

REFERENCES

Armas L. F. de & Teruel R. 2012. — Revisión del género *Microtityus* Kjellesvig-Waering, 1966 (Scorpiones: Buthidae) en República Dominicana. *Revista Ibérica de Aracnología* 21: 69-88.

Astrin J. J., Höfer H., Spelda J., Holstein J., Bayer S., Hendrich L., Huber B. A., Kielhorn K.-H., Krammer H.-J. & Lemke M. 2016. — Towards a DNA barcode reference database for spiders and harvestmen of Germany. *PLoS ONE* 11 (9): e0162624. https://doi.org/10.1371/journal.pone.0162624

Botero-Trujillo R., Erazo-Moreno M. C. & Pérez G. A. 2009. — A new species of *Microtityus* Kjellesvig-Waering (Scorpiones: Buthidae) from northern Colombia. *Zootaxa* 38 (2120): 27-38. https://doi.org/10.11646/zootaxa.2120.1.4

Botero-Trujillo R. & Flórez D. E. 2011. — A revisionary approach of Colombian *Ananteris* (Scorpiones, Buthidae): two new species, a new synonymy, and notes on the value of trichobothria and hemispermatophore for the taxonomy of the group. *Zootaxa* 44 (2904): 1-44. https://doi.org/10.11646/zootaxa.2904.1.1

Botero-Trujillo R. & Noriega J. A. 2008. — First record of the scorpion genus *Microtityus* from Colombia, with the description of a new species (Scorpiones, Buthidae). *Journal of Arachnology* 36 (2): 259-266. https://doi.org/10.1636/CH07-76.1

Bücherl W. 1956. — Escorpiões e escorpionismo no Brasil. V. Observações sobre o aparelho reprodutor masculino e o acasalamento de *Tityus trivittatus* e *Tityus bahiensis*. *Memorias do Instituto Butantan* 27: 121-155.

Crews S. C. & Esposito L. A. 2020. — Towards a synthesis of the Caribbean biogeography of terrestrial arthropods. *BMC Evolutionary Biology* 20: 1-27. https://doi.org/10.1186/s12862-019-1576-z

Crowther T. W., Glick H. B., Covey K. R., Bettigole C., Maynard D. S., Thomas S. M., Smith J. R., Hintler G., Duguid M. C. & Amatulli G. 2015. — Mapping tree density at a global scale. *Nature* 525 (7568): 201-205. https://doi.org/10.1038/nature14967

Esposito L. A. & Prendini L. 2019. — Island ancestors and New World biogeography: a case study from the scorpions (Buthidae: Centruroidinae). *Scientific Reports* 9 (1): 1-11. https://doi.org/10.1038/s41598-018-33754-8

Esposito L. A., Yamaguti H. Y., Pinto-da-Rocha R. & Prendini L. 2018. — Plucking with the plectrum: phylogeny of the New World buthid scorpion subfamily Centruroidinae Kraus, 1955 (Scorpiones: Buthidae) reveals evolution of three pecten-sternite stridulation organs. *Arthropod Systematics and Phylogeny* 76 (1): 87-122.

Esposito L. A., Yamaguti H. Y., Souza C. A., Pinto-da-Rocha R. & Prendini L. 2017. — Systematic revision of the neotropical club-tailed scorpions, *Physoctonus, Rhopalurus*, and *Troglorhopalurus*, revalidation of *Heteroctenus*, and Descriptions of Two New Genera and Three New Species (Buthidae: Rhopalurusinae). *Bulletin of the American Museum of Natural History* 415: 1-136. https://doi.org/10.1206/0003-0090-415.1.1

Fet V. & Lowe G. 2000. — Family Buthidae C. L. Koch, 1837, *Catalog of the Scorpions of the World*. The New York Entomological Society, New York: 54-286.

Fetzner Jr J. W. 1999. — Extracting high-quality DNA from shed reptile skins: a simplified method. *Biotechniques* 26 (6): 1052-1054. https://doi.org/10.2144/99266bm09

Francke O. F. & Stockwell S. A. 1987. — *Scorpions (Arachnida) from Costa Rica*. Special Publications The Museum of Texas Tech University, Austin: 1-63 (25).

Francke O. F., Teruel R. & Santibáñez-López C. E. 2014. — A new genus and a new species of scorpion (Scorpiones: Buthidae) from southeastern Mexico. *Journal of Arachnology* 42 (3): 220-232. https://doi.org/10.1636/ha13-33.1

González-Sponga M. A. 2001. — Arácnidos de Venezuela. Seis nuevas especies del género *Microtityus* (Scorpionida: Buthidae) del sistema montañoso de la costa. *Boletín de la Academía de Ciencias Físicas, Matemáticas y Naturales* LXI (1-2): 45-66.

González-Sponga M. A. 2009. — Biodiversidad en Venezuela. arácnidos. Descripción de cuatro nuevas especies del género *Tityus* Koch, 1836 (Escorpiones: Buthidae) de los Estados Bolívar y Amazonas. *Revista de Investigación* 1836 (66): 227-255.

Hoorn C., Guerrero J., Sarmiento G. A. & Lorente M. A. 1995. — Andean tectonics as a cause for changing drainage patterns in Miocene northern South America. *Geology* 23 (3): 237-240. https://doi.org/10.1130/0091-7613(1995)023<0237:ATAACF>2.3.CO;2

Hughes A. C., Orr M. C., Ma K., Costello M. J., Waller J., Provoost P., Yang Q., Zhu C. & Qiao H. 2021. — Sampling biases shape our view of the natural world. *Ecography* 44 (9): 1259-1269. https://doi.org/10.1111/ecog.05926

Kjellesvig-Waering E. N. 1966. — Scorpions of Trinidad and Tobago. *Caribbean Journal of Science* 6 (3-4): 123-135.

Kovařík F., Teruel R., Lowe G. & Friedrich S. 2015. — Four new scorpion species (Scorpiones: Buthidae) from Amazonian Peru. *Euscorpius* 210: 1-40. https://doi.org/10.18590/euscorpius.2014.vol2014.iss187.1

Kovařík F., Teruel R. & Lowe G. 2016. — Two new scorpions of the genus *Chaneke* Francke, Teruel et Santibáñez-López, 2014 (Scorpiones: Buthidae) from southern Mexico. *Euscorpius* 218: 1-20. https://doi.org/10.18590/euscorpius.2016.vol2016.iss218.1

Lenarducci Â. R. I. P., Pinto-da-Rocha R. & Lucas S. M. 2005. — Descrição de uma nova espécie de *Rhopalurus* Thorell, 1876 (Scorpiones: Buthidae) do nordeste brasileiro. *Biota Neotropica* 5 (1a): 173-180. https://doi.org/10.1590/s1676-06032005000200015

Loria S. F. & Prendini L. 2014. — Homology of the lateral eyes of scorpiones: a six-ocellus model. *PLoS ONE* 9 (12): 1-30. https://doi.org/10.1371/journal.pone.0112913

Lourenço W. R. 2004. — The genus *Ananteris* Thorell (Scorpiones, Buthidae) in the Brazilian Amazonia. *Revista Ibérica de Aracnología* 9: 137-140.

Lourenço W. R. 2005. — Scorpion diversity and endemism in the Rio Negro of Brazilian Amazonia, with the description of two new species of *Tityus* C. L. Koch (Scorpiones, Buthidae). *Amazoniana* 18 (3): 203-213.

Lourenço W. R. 2016. — Scorpions from the Mitaraka Massif in French Guiana: Description of one new genus and species (Scorpiones: Chactidae). *Comptes Rendus - Biologies* 339 (3-4): 141-146. https://doi.org/10.1016/j.crvi.2016.02.003

Lourenço W. R. 2017. — Scorpions from Brazilian Amazonia,

with a description of two new species from 'Serra da Mocidade' National Park in the State of Roraima (Scorpiones: Buthidae, Chactidae). *Arachnida - Rivista Aracnologica Italiana* 12: 2-17
Lourenço W. R. & Duhem B. 2009. — The genus *Vachoniochactas* González-Sponga (Scorpiones, Chactidae), a model of relictual distribution in past refugia of the Guayana region of South America. *Comptes Rendus - Biologies* 332 (12): 1085-1091. https://doi.org/10.1016/j.crvi.2009.09.006
Lourenço W. R. & Duhem B. 2010. — Further considerations on the genus *Ananteris* Thorell, 1891 (Scorpiones, Buthidae) in Brazilian Amazonia and description of two new species. *Boletín de la Sociedad Entomológica Aragonesa* (47): 33-38.
Lourenço W. & Eickstedt V. R. D. V. 1983. — Présence du genre *Microtityus* (Scorpiones, Buthidae) au Brésil. Description de *Microtityus vanzolinii* sp. n. *Revue Arachnologique* 5 (2): 65-72.
Lourenço W. R., Giupponi A. & Pedroso D. R. 2011. — New species of Chactidae (Scorpiones) from the Upper Rio Negro in Brazilian Amazonia. *Revista Ibérica de Aracnología* 49: 65-75.
Lovejoy N. R., Bermingham E. & Martin A. P. 1998. — Marine incursion into South America. *Nature* 396 (6710): 421-422. https://doi.org/10.1038/24757
Matthiesen F. A. 1976. — *O escorpião*. São Paulo, Edart, 72 p.
Matthiesen F. A. 1968. — On the male reproductive organs in some Brazilian scorpions. *Revista Brasileira de Pesquisas Médicas e Biológicas* 1: 273-274.
Merow C., Smith M. J. & Silander Jr J. A. 2013. — A practical guide to MaxEnt for modeling species' distributions: what it does, and why inputs and settings matter. *Ecography* 36 (10): 1058-1069. https://doi.org/10.1111/j.1600-0587.2013.07872.x
Miranda R. J. & Armas L. F. de 2020. — A new species of *Ananteris* (Scorpiones: Buthidae) from Panama. *Euscorpius* 297: 1-7.
Monod L., Cauwet L., González-Santillán E. & Huber S. 2017. — The male sexual apparatus in the order Scorpiones (Arachnida): A comparative study of functional morphology as a tool to define hypotheses of homology. *Frontiers in Zoology* 14 (1): 1-48. https://doi.org/10.1186/s12983-017-0231-z
Moreno-González J. A., González-Obando R. & Flórez D. A. 2019. — Taxonomic revision of the Colombian *Tityus* (*Archaeotityus*) (Scorpiones, Buthidae) species: a morphological and morphometric approach, with a description of a new species. *Zootaxa* 4660 (1): 1-94. https://doi.org/10.11646/zootaxa.4660.1.1
Moreno-González J. A., Pinto-Da-Rocha R. & Cabra-García J. J. 2022. — On the *Tityus forcipula* species group: redescription of *Tityus forcipula* (Scorpiones, Buthidae), description of a new Andean species, and notes on the taxonomy of the group. *Zootaxa* 5155 (2): 151-186. https://doi.org/10.11646/zootaxa.5155.2.1
Morrone J. J. 2017. — *Neotropical biogeography: regionalization and evolution*. Boca Raton, CRC Press, Taylor & Francis Group, 282 p.
Ochoa J. A., Botero-Trujillo R. & Prendini L. 2010. — On the troglomorphic scorpion *Troglotayosicus humiculum* (Scorpiones, Troglotayosicidae), with first description of the adults. *American Museum Novitates* 3691: 1-19. https://doi.org/10.1206/707.1
Ojanguren-Affilastro A. A. 2005. — Estudio monográfico de los escorpiones de la República Argentina. *Revista Ibérica de Aracnología* 11: 75-246.
Ojanguren-Affilastro A. A., Adilardi R. S., Cajade R., Ramírez M. J., Ceccarelli F. S. & Mola L. M. 2017. — Multiple approaches to understanding the taxonomic status of an enigmatic new scorpion species of the genus *Tityus* (Buthidae) from the biogeographic island of Paraje Tres Cerros (Argentina). *PLoS ONE* 12 (7): 1-24. https://doi.org/10.1371/journal.pone.0181337
Oliveira U., Paglia A. P., Brescovit A. D., de Carvalho C. J., Silva D. P., Rezende D. T., Leite F. S.F., Batista J. A.N., Barbosa J. P.P. P. & Stehmann J. R. 2016. — The strong influence of collection bias on biodiversity knowledge shortfalls of Brazilian terrestrial biodiversity. *Diversity and Distributions* 22 (12): 1232-1244. https://doi.org/10.1111/ddi.12489
Oliveira U., Soares-Filho B. S., Paglia A. P., Brescovit A. D., de Carvalho C. J., Silva D. P., Rezende D. T., Leite F. S. F., Batista J. A. N. & Barbosa J. P. P. P. 2017. — Biodiversity conservation gaps in the Brazilian protected areas. *Scientific Reports* 7 (1): 9141. https://doi.org/10.1038/s41598-017-08707-2
Oliveira U., Soares-Filho B., Leitão R. F. M. & Rodrigues H. O. 2019. — BioDinamica: a toolkit for analyses of biodiversity and biogeography on the Dinamica-EGO modelling platform. *PeerJ* 7: e7213. https://doi.org/10.7717/peerj.7213
Pinto-da-Rocha R., Bragagnolo C., Marques F. P. & Antunes Junior M. 2014. — Phylogeny of harvestmen family Gonyleptidae inferred from a multilocus approach (Arachnida: Opiliones). *Cladistics* 30 (5): 519-539. https://doi.org/10.1111/cla.12065
Prendini L. 2000. — Phylogeny and classification of the superfamily Scorpionoidea Latreille 1802 (Chelicerata, Scorpiones): An exemplar approach. *Cladistics* 16 (1): 1-78. https://doi.org/10.1111/j.1096-0031.2000.tb00348.x
Prendini L., Esposito L. A., Huff J. C. & Volschenk E. S. 2009. — Redescription of *Rhopalurus abudi* (Scorpiones, Buthidae), with first description of the male and first record from mainland Hispaniola. *Journal of Arachnology* 37: 206-224. https://doi.org/10.1636/H08-55.1
Rojas-Runjaic F. J. M. & Sousa L. de D. 2007. — Catálogo de los escorpiones de Venezuela (Arachnida: Scorpiones). *Boletín Sociedad Entomológica Aragonesa* 40: 281-307.
Santos M. D. S. dos, Porto T. J., Lira-da-Silva R. M. & Brazil T. K. 2014. — Description of the male of *Tityus kuryi* Lourenço, 1997 and notes about males of *Tityus stigmurus* (Thorell, 1877) and *Tityus serrulatus* Lutz & Mello, 1922 (Scorpiones, Buthidae). *ZooKeys* 61: 49-61. https://doi.org/10.3897/zookeys.435.6694
Santos-da-Silva A. de P., Carvalho L. S. & Brescovit A. D. 2017. — Two new species of *Bothriurus* Peters, 1861 (Scorpiones, Bothriuridae) from Northeastern Brazil. *Zootaxa* 4258 (3): 238-256. https://doi.org/10.11646/zootaxa.4258.3.2
Schawaller W. 1982. — Zwei weitere Skorpione in Dominikanischem Berstein (Stuttgarter Bernsteinsammlung: Arachnida; Scorpionida). *Stuttgarter Beiträge zur Naturkunde* 82: 1-14.
Simard M., Pinto N., Fisher J. B. & Baccini A. 2011. — Mapping forest canopy height globally with spaceborne lidar. *Journal of Geophysical Research: Biogeosciences* 116 (G4). https://doi.org/10.1029/2011JG001708
Sissom W. D. 1990. — *Systematics, Biogeography, and Paleontology, The Biology of Scorpions*. California, Standford University Press: 31-80.
Sissom W. D., Polis G. A. & Watt D. D. 1990. — *Field and laboratory methods, The Biology of Scorpions*. California, Standford University Press: 445-461.
Soleglad M. E. & Fet V. 2003. — The scorpion sternum: structure and phylogeny (Scorpiones: Orthosterni). *Euscorpius* 5: 1-34. https://doi.org/10.18590/euscorpius.2003.vol2003.iss5.1
Stahnke H. L. 1970. — Scorpion nomenclature and mensuration. *Entomological News* 81: 297-316.
Stockwell S. A. 1989. — *Revision of the phylogeny and higher classification of scorpions (Chelicerata)* Ph. D. thesis. University of California at Berkeley, Berkeley, 413 p.
Teruel R. & Armas L. F. de 2012. — Redescripción de *Rhopalurus junceus* (Herbst 1800) (Scorpiones: Buthidae). *Boletín de la Sociedad Entomológica Aragonesa* 50: 53-74.
Teruel R. & Kovařík F. 2012. — *Scorpions of Cuba*. Czech Republic, Jakub Rolcik- Clarion Production, 229 p.
Vachon M. 1963. — De l'utilité, en systématique, d'une nomenclature des dents des chélicères chez les Scorpions. *Bulletin du Muséum national d'Histoire naturelle* (2): 161-166. https://www.

biodiversitylibrary.org/partpdf/250792

VACHON M. 1975. — Sur l'utilisation de la trichobothriotaxie du bras des pédipalpes des Scorpions (Arachnides) dans le classement des genres de la famille des Buthidae Simon. *Comptes Rendus des séances de l'Académie des Sciences, série D* 281: 1597-1599.

VACHON M. 1974. — Étude des caractères utilisés pour classer les familles et les genres de Scorpions (Arachnides). 1. La trichobothriotaxie en arachnologie. Sigles trichobothriaux et types de trichobothriotaxie chez les Scorpions. *Bulletin du Muséum national d'Histoire naturelle* 140: 857-958.

WEBB S. D. 1995. — Biological implications of the middle Miocene Amazon seaway. *Science* 269 (5222): 361-362. https://doi.org/10.1126/science.269.5222.361

YTHIER E. 2019. — A new species of *Megachactops* Ochoa, Rojas-Runjaic, Pinto-da-Rocha and Prendini, 2013 (Scorpiones: Chactidae) from Colombia. *Revista Ibérica de Aracnología* 34: 69-75.

Submitted on 26 April 2023;
accepted on 10 November 2023;
published on 25 April 2024.

APPENDICE

APPENDIX 1. — Records of *Microtityus* Kjellesvig-Waering, 1966 species used in the present study.

Taxa	Country	Origin of the coordinates	Latitude	Longitude
Microtityus adriki n. sp.	Brazil	GPS coordinates	2.588	–60.641
Microtityus adriki n. sp.	Brazil	GPS coordinates	2.614	–60.608
Microtityus aff. dominicanensis	Dominican Republic	Google Earth, approximate	18.725	–70.455
Microtityus angelaerrosae	Venezuela	Original publication	10.054	–63.701
Microtityus barahona	Dominican Republic	Google Earth, approximate	18.130	–71.066
Microtityus barahona	Dominican Republic	Google Earth, approximate	18.327	–71.572
Microtityus biordi	Venezuela	Rojas-Runjaic & De Sousa (2007)	10.456	–66.472
Microtityus bivicentorum	Colombia	Original publication	10.574	–73.263
Microtityus bivicentorum	Colombia	Original publication	10.574	–73.274
Microtityus borincanus	Puerto Rico	Original publication	18.093	–66.909
Microtityus capayaensis	Venezuela	Original publication	10.431	–66.271
Microtityus consuelo	Dominican Republic	Google Earth, approximate	18.434	–68.966
Microtityus consuelo	Dominican Republic	Google Earth, approximate	18.807	–69.785
Microtityus consuelo	Dominican Republic	Google Earth, approximate	18.400	–69.100
Microtityus desuzeae	Venezuela	Original publication	9.424	–67.269
Microtityus difficilis	Cuba	Original publication	20.639	–75.029
Microtityus difficilis	Cuba	Original publication	20.668	–74.973
Microtityus difficilis	Cuba	Original publication	20.621	–74.878
Microtityus difficilis	Cuba	Original publication	20.668	–74.973
Microtityus difficilis	Cuba	Original publication	20.668	–74.973
Microtityus dominicanensis	Dominican Republic	Google Earth, approximate	18.424	–70.033
Microtityus dominicanensis	Dominican Republic	Google Earth, approximate	18.725	–70.455
Microtityus dominicanensis	Dominican Republic	Google Earth, approximate	18.424	–70.033
Microtityus eustatia	British Virgin Islands	Original publication	18.512	–64.356
Microtityus eustatia	British Virgin Islands	Original publication	18.482	–64.389
Microtityus eustatia	British Virgin Islands	Original publication	18.475	–64.532
Microtityus eustatia	British Virgin Islands	Original publication	18.470	–64.531
Microtityus farleyi	Cuba	Google Earth, approximate	20.253	–74.173
Microtityus farleyi	Cuba	Google Earth, approximate	20.253	–74.173
Microtityus farleyi	Cuba	Google Earth, approximate	20.253	–74.173
Microtityus farleyi	Cuba	Google Earth, approximate	20.253	–74.173
Microtityus flavescens	Cuba	Google Earth, approximate	19.973	–75.874
Microtityus flavescens	Cuba	Google Earth, approximate	19.973	–75.874
Microtityus flavescens	Cuba	Google Earth, approximate	19.973	–75.874
Microtityus flavescens	Cuba	Google Earth, approximate	19.973	–75.874
Microtityus flavescens	Cuba	Google Earth, approximate	19.973	–75.874
Microtityus flavescens	Cuba	Google Earth, approximate	19.973	–75.874
Microtityus flavescens	Cuba	Google Earth, approximate	19.973	–75.874
Microtityus franckei	Colombia	Original publication	11.273	–74.083
Microtityus franckei	Colombia	Original publication	11.273	–74.083
Microtityus fundorai	Cuba	Google Earth, approximate	20.651	–75.685
Microtityus fundorai	Cuba	Google Earth, approximate	20.651	–75.685
Microtityus fundorai	Cuba	Google Earth, approximate	20.062	–75.942
Microtityus fundorai	Cuba	Google Earth, approximate	20.062	–75.942
Microtityus fundorai	Cuba	Google Earth, approximate	20.043	–75.817
Microtityus fundorai	Cuba	Google Earth, approximate	20.043	–75.817
Microtityus fundorai	Cuba	Google Earth, approximate	20.043	–75.817
Microtityus fundorai	Cuba	Google Earth, approximate	19.962	–75.783
Microtityus fundorai	Cuba	Google Earth, approximate	20.013	–75.638
Microtityus fundorai	Cuba	Google Earth, approximate	20.013	–75.638
Microtityus fundorai	Cuba	Google Earth, approximate	20.013	–75.638
Microtityus fundorai	Cuba	Google Earth, approximate	20.013	–75.638
Microtityus guantanamo	Cuba	Google Earth, approximate	20.500	–75.083
Microtityus iviei	Dominican Republic	Google Earth, approximate	18.075	–71.657
Microtityus iviei	Dominican Republic	Google Earth, approximate	18.121	–71.455
Microtityus iviei	Dominican Republic	Google Earth, approximate	18.121	–71.455
Microtityus iviei	Dominican Republic	Google Earth, approximate	18.155	–71.745
Microtityus iviei	Dominican Republic	Google Earth, approximate	17.906	–71.502
Microtityus iviei	Dominican Republic	Google Earth, approximate	17.822	–71.433
Microtityus iviei	Dominican Republic	Google Earth, approximate	17.801	–71.340
Microtityus iviei	Dominican Republic	Google Earth, approximate	17.786	–71.501
Microtityus jaumei	Cuba	Google Earth, approximate	19.968	–75.869
Microtityus jaumei	Cuba	Google Earth, approximate	19.968	–75.869
Microtityus jaumei	Cuba	Google Earth, approximate	19.968	–75.869
Microtityus jaumei	Cuba	Original publication	20.162	–75.363
Microtityus joseantonioi	Venezuela	Rojas-Runjaic & De Sousa (2007)	10.058	–65.400
Microtityus kovariki	Cuba	Original publication	20.276	–76.562

Appendix 1. — Continuation.

Taxa	Country	Origin of the coordinates	Latitude	Longitude
Microtityus kovariki	Cuba	Original publication	20.276	–76.562
Microtityus kovariki	Cuba	Original publication	20.276	–76.562
Microtityus kovariki	Cuba	Original publication	20.276	–76.562
Microtityus kovariki	Cuba	Original publication	20.276	–76.562
Microtityus kovariki	Cuba	Original publication	20.276	–76.562
Microtityus kovariki	Cuba	Original publication	20.276	–76.562
Microtityus kovariki	Cuba	Original publication	20.276	–76.562
Microtityus kovariki	Cuba	Original publication	20.276	–76.562
Microtityus kovariki	Cuba	Original publication	20.276	–76.562
Microtityus kovariki	Cuba	Original publication	20.276	–76.562
Microtityus kovariki	Cuba	Original publication	20.276	–76.562
Microtityus kovariki	Cuba	Original publication	20.276	–76.562
Microtityus kovariki	Cuba	Original publication	20.276	–76.562
Microtityus kovariki	Cuba	Original publication	20.276	–76.562
Microtityus latinguai	Dominican Republic	Google Earth, approximate	17.786	–71.501
Microtityus latinguai	Dominican Republic	Google Earth, approximate	17.570	–71.513
Microtityus litoralensis	Venezuela	Original publication	10.567	–67.153
Microtityus lourencoi	Dominican Republic	Google Earth, approximate	18.350	–68.828
Microtityus lourencoi	Dominican Republic	Google Earth, approximate	18.350	–68.828
Microtityus minimus	Dominican Republic	Original publication	18.355	–70.515
Microtityus minimus	Dominican Republic	Original publication	18.355	–70.515
Microtityus paucidentatus	Dominican Republic	Google Earth, approximate	18.581	–71.415
Microtityus paucidentatus	Dominican Republic	Google Earth, approximate	18.581	–71.415
Microtityus prendinii	Dominican Republic	Google Earth, approximate	19.282	–69.203
Microtityus prendinii	Dominican Republic	Google Earth, approximate	19.282	–69.203
Microtityus prendinii	Dominican Republic	Google Earth, approximate	19.229	–69.613
Microtityus pusillus	Cuba	Original publication	19.955	–76.757
Microtityus pusillus	Cuba	Original publication	19.955	–76.757
Microtityus pusillus	Cuba	Original publication	19.955	–76.757
Microtityus pusillus	Cuba	Original publication	19.955	–76.757
Microtityus pusillus	Cuba	Original publication	19.955	–76.757
Microtityus pusillus	Cuba	Original publication	19.955	–76.757
Microtityus reini	Dominican Republic	Google Earth, approximate	18.334	–70.328
Microtityus reini	Dominican Republic	Google Earth, approximate	18.352	–70.335
Microtityus reini	Dominican Republic	Google Earth, approximate	18.352	–70.335
Microtityus reini	Dominican Republic	Google Earth, approximate	18.352	–70.335
Microtityus rickyi	Trinidad	Google Earth, approximate	10.686	–61.661
Microtityus rickyi	Trinidad	Google Earth, approximate	10.686	–61.661
Microtityus rickyi	Trinidad	Google Earth, approximate	10.686	–61.661
Microtityus rickyi	Trinidad	Google Earth, approximate	10.686	–61.661
Microtityus rickyi	Trinidad	Google Earth, approximate	10.686	–61.661
Microtityus rickyi	Trinidad	Google Earth, approximate	10.686	–61.661
Microtityus rickyi	Trinidad	Google Earth, approximate	10.686	–61.661
Microtityus rickyi	Trinidad	Google Earth, approximate	10.686	–61.661
Microtityus rickyi	Trinidad and Tobago	Google Earth, approximate	10.686	–61.510
Microtityus rickyi	Trinidad	Original publication	10.664	–61.399
Microtityus rickyi	Trinidad	Google Earth, approximate	10.666	–61.655
Microtityus rickyi	Tobago	Original publication	11.306	–60.538
Microtityus rickyi	Tobago	Google Earth, approximate	11.298	–60.502
Microtityus santosi	Puerto Rico	Original publication	18.093	–66.909
Microtityus sevciki	Venezuela	Original publication	10.234	–68.780
Microtityus sevciki	Venezuela	Google Earth, approximate	10.460	–67.733
Microtityus solegladi	Dominican Republic	Google Earth, approximate	18.581	–71.415
Microtityus solegladi	Dominican Republic	Google Earth, approximate	18.749	–70.837
Microtityus sp.	Dominican Republic	Google Earth, approximate	18.075	–71.657
Microtityus sp.	Dominican Republic	Google Earth, approximate	17.906	–71.502
Microtityus sp.	Dominican Republic	Google Earth, approximate	17.822	–71.433
Microtityus sp.	Dominican Republic	Google Earth, approximate	17.786	–71.501
Microtityus sp.	Dominican Republic	Google Earth, approximate	19.207	–70.983
Microtityus starri	Trinidad and Tobago	Google Earth, approximate	11.298	–60.502
Microtityus starri	Trinidad and Tobago	Google Earth, approximate	11.298	–60.502
Microtityus starri	Trinidad and Tobago	Google Earth, approximate	11.298	–60.502
Microtityus trinitensis	Cuba	Google Earth, approximate	22.072	–80.465
Microtityus trinitensis	Cuba	Google Earth, approximate	21.915	–80.019
Microtityus trinitensis	Cuba	Google Earth, approximate	21.801	–80.010
Microtityus vanzolinii	Brazil	Google Earth, approximate	–2.347	–64.838
Microtityus vieques	Puerto Rico	Google Earth, approximate	18.093	–65.552
Microtityus virginiae	Dominican Republic	Google Earth, approximate	18.639	–71.649
Microtityus vulcanicus	Cuba	Original publication	19.937	–75.274
Microtityus vulcanicus	Cuba	Original publication	19.940	–75.314

Appendix 1. — Continuation.

Taxa	Country	Origin of the coordinates	Latitude	Longitude
Microtityus vulcanicus	Cuba	Original publication	19.937	–75.274
Microtityus vulcanicus	Cuba	Original publication	19.914	–75.244
Microtityus waeringi	United States	Google Earth, approximate	18.337	–64.728
Microtityus waeringi	United States	Google Earth, approximate	18.318	–64.732
Microtityus waeringi	United States	Google Earth, approximate	18.321	–64.855
Microtityus yaracuyanus	Venezuela	Rojas-Runjaic & De Sousa (2007)	10.180	–68.625